
Efficient Decision Making and Belief Space Planning using Sparse Approximations

Khen Elimelech¹ and Vadim Indelman²

¹Robotics and Autonomous Systems Program

²Faculty of Aerospace Engineering

Technion - Israel Institute of Technology, Haifa, 3200003, Israel

Abstract

In this work, we introduce a new approach for the efficient solution of autonomous decision and planning problems, with a special focus on decision making under uncertainty and belief space planning (BSP) in high-dimensional state spaces. Usually, to solve the decision problem, we identify the optimal action, according to some objective function. Instead, we claim that we can sometimes generate and solve an analogous yet simplified decision problem, which can be solved more efficiently. Furthermore, a wise simplification method can lead to the same action selection, or one for which the maximal loss can be guaranteed. This simplification is separated from the state inference, and does not compromise its accuracy, as the selected action would finally be applied on the original state. At first, we develop the concept for general decision problems, and provide a theoretical framework of definitions to allow a coherent discussion. We then practically apply these ideas to BSP problems, in which the problem is simplified by considering a sparse approximation of the initial belief. The scalable sparsification algorithm we provide is able to yield solutions which are guaranteed to be consistent with the original problem. We demonstrate the benefits of the approach in the solution of a highly realistic active-SLAM problem, and manage to significantly reduce computation time, with practically no loss in the quality of solution. This rigorous and fundamental work is conceptually novel, and holds numerous possible extensions.

1 Introduction

1.1 Background

In this era, intelligent autonomous agents and robots can be found all around us. They are designed for various functions, such as operating in remote domains, e.g. underwater and space; imitating humans and interacting with them; performing repetitive tasks; and ensuring safety of operations. They might be physically noticeable, e.g. personal-use drones, industrial robotic arms, or military vehicles; or less so, with the popularization of internet of things (IoT), smart homes, and virtual assistants. These agents share the same fundamental goal – to autonomously plan and execute their actions. Yet, the increasing demand for these “smart” systems presents new challenges. Integration of robotic agents into everyday life requires them to efficiently operate using inexpensive hardware.

In addition, when planning their actions, these agents should account for real-world uncertainty in order to achieve reliable and robust performance. There are multiple possible sources for such uncertainty, including dynamic environments, in which unpredictable events might occur; noisy or limited observations, such as an imprecise GPS signal; and inaccurate delivery of actions. Also, problems, such as long-term autonomous navigation and sensor placement over large areas, often involve optimization of numerous variables. These settings require reasoning over high-dimensional probabilistic states, known as “beliefs”.

Appropriately, the corresponding planning problem is known as Belief Space Planning (BSP). Relevant instantiations include active Simultaneous Localization and Mapping (SLAM), sensor placement and active sensing, robotic arm manipulation, and recently more profound problems, such as dialogue management. The objective in such problems is to select “safe” actions, which reduce the uncertainty of the agent’s belief.

The BSP problem is often modeled as a Partially Observable Markov Decision Process (POMDP), according to which we evaluate the propagation of uncertainty, considering *multiple* courses of action. Yet, proper uncertainty measures, such as differential entropy, are expensive to calculate. Overall, the computational complexity of the problem can turn exceptionally high, thus making it challenging for online systems, or when having a limited processing power. In fact, the optimal solution of a POMDP was proven to be intractable (Papadimitriou and Tsitsiklis 1987). It should be stated, though, that not every planning problem can fit this model, with the most obvious example being a non-Markovian scenario.

1.2 Objectives and Approach Overview

In this study, we differentiate between planning and decision problems. Planning is a broad concept, which takes into

consideration many aspects, such as goal setting, definition of actions, accounting for different planning horizons and future developments, coordination of agents, and so on. After refining these aspects, we eventually result in a decision problem: considering an initial state, and a *given* set of candidate actions (or action sequences), we use an objective function to measure the scalar values attained by applying each action on the initial state. To solve the problem, we wish to identify the optimal candidate action, which generates the highest objective function value. This discussion leads us to our main goal – allowing computationally efficient decision making. With this rudimentary view-point, we dismiss problem-specific attributes, which allows us to address a wider range of problems with our formulation. Nonetheless, our work heavily focuses on contributing to the solution of high-dimensional BSP problems, in which the initial state is a belief, and the objective function measures the expected cumulative reward, gained by applying some action.

A traditional solution to such decision problem requires calculation of the objective function for each candidate action. We would like to reduce the cost of the solution by sparing this exhaustive calculation. Instead, we suggest to identify and solve a simplified problem, which leads to the same action selection, or for which the loss in quality of solution can be bounded. A problem may be simplified by adapting each of its components – initial state, objective function, and candidate actions. After solving the decision problem, the selected action is then applied on the *original* state. To allow such analysis, we first provide a theoretical framework of appropriate definitions and theorems, which does not depend on any problem-specific attributes. We then show how these general ideas can be practically applied to high-dimensional BSP problems. In this case, the problem is simplified using a sparse approximation of the initial belief. The simplified problem itself can be solved in any desired manner, making our approach complementary to other solution methods. Furthermore, while several works already utilize belief sparsification to allow long-term operation and state inference, the novelty in our approach is the exploitation of sparse approximations exclusively for efficient decision making; the state inference process notably remains untouched and exact. For clarity, we list down the new contributions presented here:

1. Formulation of the novel concept of problem simplification for efficient decision making;
2. Extended formulation for the application of the concept for BSP problems;
3. An improved belief sparsification algorithm;
4. Derivation of quality of solution bounds for simplified BSP problems;
5. Usage demonstration in a highly realistic active-SLAM scenario, where a significant improvement in run-time is achieved.

Please note that this paper extends our previous publications (Elimelech and Indelman 2017*a,b,c*), and includes several revisions and corrections to previously introduced definitions. The conclusive versions are those presented here. Also, to allow fluid reading, proofs for all theorems and corollaries are given in the appendix.

1.3 Related Work

Several works explore similar ideas to the ones presented here. In this section we do our best to provide an extensive review of such works, in comparison to ours.

As mentioned, numerous methods consider sparsification for the state inference problem, in order to limit the state size and allow long-term operation. Although being a well researched concept, these methods do not examine sparsification in the context of planning problems (influence over action selection, computational benefits, etc.). Thrun et al. (2004), for example, showed that in a SLAM scenario, when using the information filter, forcing a certain sparsity pattern on the information matrix can lead to improved efficiency in belief update. However, they emphasized that the approximation quality was not guaranteed and that certain scenarios could lead to significant divergence. Additionally, graph-based solutions for SLAM problems have become more popular in recent years (Dellaert and Kaess 2006); in parallel, methods for graph sparsification have also gained relevance. Huang et al. (2012) introduced a graph sparsification method, using node marginalization. The resulted graph is notably consistent, meaning, the sparsified representation is not more confident than the original one. Several other approaches suggest to sparsify the graph using the Chow-Liu tree approximation, and show that the KL-divergence from the original graph remains low (Carlevaris-Bianco et al. 2014; Carlevaris-Bianco and Eustice 2014; Kretzschmar and Stachniss 2012). Hsiung et al. (2018) reach similar conclusions for fixed-lag Markov blankets. The approach described by Mu et al. (2017) separated the sparsification into two stages: problem-specific removal of nodes, and problem-agnostic removal of correlations. The authors then demonstrated the superiority of their scheme over agnostic graph optimization, in terms of collision percentage. This two-stage solution reminds the logic in our sparsification method: first, identifying variables with minimal contribution to the decision problem, and then sparsification of corresponding elements. Of course, we use such sparsification for planning and not for graph optimization. Exploiting sparsity to improve efficiency can also be done in other manners. Fundamental works (e.g. Davis et al. 2004), alongside newer ones (e.g. Frey et al. 2017), provide heuristics for variable ordering or variable pruning order, in order to minimize fill-in during factorization.

In the context of POMDP, the research community has been extensively investigating solution methods to provide better scalability in real-world problems. As mentioned, our approach is complementary to such methods, which can be used when solving the simplified BSP problem. General methods include, for example, point-based value iteration (e.g. Porta et al. 2006; Pineau et al. 2006), sampling-based motion planning (e.g. Prentice and Roy 2009; Karaman and Frazzoli 2011; Kavraki et al. 1996), and direct trajectory optimization approaches (e.g. Indelman et al. 2015; Van Den Berg et al. 2012). Approaches that focus on autonomous navigation problems, such as active SLAM, have been also widely examined (e.g. Stachniss et al. 2004; Bryson and Sukkarieh 2008; Du et al. 2011; Kim and Eustice 2014; Chaves and Eustice 2016; Kopitkov and Indelman 2017).

More closely related to our approach, several other works examine approximation of the state or the objective function in order to reduce the planning complexity. A recent approach (Bopardikar et al. 2016) suggested using a bound over the maximal eigenvalue of the covariance matrix as a cost function for planning, in an autonomous navigation scenario. Benefits of using this cost function include easy computation, holding an optimal substructure property (incremental search) and the ability to account to misdetection of measurements. Yet, the actual quality of results in terms of final uncertainty, when measured in conventional methods, is unclear. Their usage of bounds in attempt to improve planning efficiency reminds aspects of our work; however, we use bounds to quantify the quality of solution. As they mention in their discussion, an unanswered question is the difference in quality of solution between planning using the exact maximal eigenvalue, and planning using its bound. Our theoretical scheme might be able to provide answer to this question. Boyen and Koller (1998) suggested maintaining an approximation of the belief for efficient state inference. This approximation is done by dividing state variables into a set number of classes, and then using a product of marginals, while treating each class of variables as a single “metavariable”. A k -class belief simplification cuts the original exponential inference complexity by a factor of k . The study showed that in rapidly-mixing POMDPs the expectation of the error could be bounded. This simplification method was later examined under a restrictive planning scenario (McAllester and Singh 1999). The planning was performed using a planning-tree search, in which a constant amount of possible observations was sampled for each tree level, and again assuming a rapidly-mixing POMDP. There, the error induced by planning in the approximated belief space can be bounded as well. This method shares similar objectives with our work, but examines a very specific scenario, which limits its generality. The approach described by Roy et al. (2005) tried to find approximate POMDP solutions through belief compression, which was done with a PCA-based algorithm. This key idea is very similar to ours, however, in that work, the objective function (i.e. decision making) still used the original decompressed belief, instead of the simplified one. Thus, no apparent computational improvement was achieved in planning complexity. The paper also did not make a comparison of this nature, and only presented analysis on the quality of compression. The work presented by Indelman (2015, 2016) contained the first explicit attempt to use belief sparsification to specifically achieve efficient planning. The papers showed that using a diagonal covariance approximation, a similar action selection could usually be maintained, while significantly reducing the complexity of the objective calculation. This claim, however, is most often not guaranteed. Optimal action selection was only proved under severely simplifying assumptions – when candidate actions and observations only update a single state variable, with a rank-1 update of the information. This attempt inspired our extensive research and in-depth, formal analysis.

It is worth mentioning that the idea of examining only the order of candidate actions (instead of their objective function value) sometimes appears in the context of economics

under the term *ordinal utility* (e.g. Manski 1988). This term, however, is not prominent in the context of artificial intelligence.

2 Efficient Decision Making: Fundamentals

2.1 Simplified Decision Problems

To begin with, let us formally define the *decision problem*.

Definition 1. Decision Problem.

A *decision problem* \mathcal{P} is a 3-tuple (ξ, \mathcal{A}, J) , where ξ is the *initial state*, from which we examine a *set of candidate actions* \mathcal{A} (finite or infinite), using an *objective function* $J: \{\xi\} \times \mathcal{A} \rightarrow \mathbb{R}$. Solving the problem means selecting the optimal action a^* , s.t.

$$a^* = \operatorname{argmax}_{a \in \mathcal{A}} J(\xi, a). \quad (1)$$

With our approach, we wish to identify and solve a simplified yet analogous decision problem $\mathcal{P}_s \doteq (\xi_s, \mathcal{A}_s, J_s)$, which results in the same (or similar) action selection, but for which the solution is more computationally efficient. Such simplification can be achieved by altering any of the problem components – initial state, candidate actions, and objective function.

Solving a simplified problem may lead to loss in the quality of solution, when the selected action is not the real optimal action. Most often it is possible to settle for a sub-optimal action selection in order to reduce the complexity of the problem; yet, to provide valuable results, it is important to quantify and bound this loss. We suggest the following measure for the accuracy of the simplification:

Definition 2. Loss.

The *loss* between a decision problem $\mathcal{P} \doteq (\xi, \mathcal{A}, J)$ and its simplification $\mathcal{P}_s \doteq (\xi_s, \mathcal{A}_s, J_s)$, due to sub-optimal action selection, is

$$\begin{aligned} \operatorname{loss}(\mathcal{P}, \mathcal{P}_s) &\doteq J(\xi, a^*) - J(\xi, a_s^*), \\ \text{where } a^* &= \operatorname{argmax}_{a \in \mathcal{A}} J(\xi, a), \quad a_s^* = \operatorname{argmax}_{a_s \in \mathcal{A}_s} J_s(\xi_s, a_s). \end{aligned} \quad (2)$$

This loss measures the difference between the maximal objective value, obtained by applying the optimal candidate action a^* on ξ , and the one obtained by applying a_s^* , which is the optimal candidate action according to the simplified problem. Clearly, when the solutions of the two problems agree, there is no loss. We implicitly assume that the original objective function J can accept and evaluate actions from the simplified set of actions \mathcal{A}_s . This idea is illustrated in Fig. 1b.

2.2 Action Consistency

We point out a key observation: to solve the decision problem, we should only *sort* the candidate actions in terms of their objective function value; changing the values themselves, without changing the order of actions, does not change the action selection. Hence, when two problems maintain the same order of candidate actions, their solution is equivalent. In this case, we can simply say that the two problems are action consistent, as demonstrated in Fig. 1a.

Definition 3. Action Consistency.

Two decision problems $\mathcal{P}_1 \doteq (\xi_1, \mathcal{A}, J_1)$, $\mathcal{P}_2 \doteq (\xi_2, \mathcal{A}, J_2)$ are *action consistent*, and marked $\mathcal{P}_1 \simeq \mathcal{P}_2$, if the following applies $\forall a_i, a_j \in \mathcal{A}$:

$$J_1(\xi_1, a_i) < J_1(\xi_1, a_j) \iff J_2(\xi_2, a_i) < J_2(\xi_2, a_j). \quad (3)$$

Note that (from now on) we consider the same set of candidate actions. If also $J_1 \equiv J_2$, we can simply say that ξ_1, ξ_2 are *action consistent*, and mark $\xi_1 \simeq \xi_2$.

Surely, if $\mathcal{P} \simeq \mathcal{P}_s$, then $\text{loss}(\mathcal{P}, \mathcal{P}_s) = 0$, as desired. Although action consistency is a more conservative demand than just zeroing the loss, this relation holds several interesting properties.

Corollary 1.

Action consistency (\simeq) is an equivalence relation, i.e. for any three decision problems $\mathcal{P}_1, \mathcal{P}_2, \mathcal{P}_3$, the following properties apply:

1. Reflexivity: $\mathcal{P}_1 \simeq \mathcal{P}_1$.
2. Symmetry: $\mathcal{P}_1 \simeq \mathcal{P}_2 \iff \mathcal{P}_2 \simeq \mathcal{P}_1$.
3. Transitivity: $\mathcal{P}_1 \simeq \mathcal{P}_2 \wedge \mathcal{P}_2 \simeq \mathcal{P}_3 \implies \mathcal{P}_1 \simeq \mathcal{P}_3$.

Corollary 1 implies that the entire space of decision problems is divided into separate equivalence-classes of action consistent problems. Theorem 1 adds that we can transfer between action consistent problems using monotonically increasing functions. We remind again that all proofs are given in Appendix A.

Theorem 1.

$\mathcal{P}_1 \simeq \mathcal{P}_2 \iff$ the mapping $f: J_1(\xi_1, a) \mapsto J_2(\xi_2, a)$ is monotonically increasing.

Meaning, if the (scalar) mapping of respective objective values between the two problems agrees with a monotonically increasing function (e.g. a constant shift, a linear transform, or a logarithmic function), then the problems are action consistent. If this mapping is not monotonically increasing, then the problems are not action consistent.

2.3 The Simplification Offset

To support the understating that action consistency indicates equivalence in the space of decision problems, we may also identify an appropriate ‘‘distance’’ measure.

Definition 4. Simplification Offset.

The *simplification offset* between a decision problem $\mathcal{P} \doteq (\xi, \mathcal{A}, J)$, and its simplification $\mathcal{P}_s \doteq (\xi_s, \mathcal{A}, J_s)$ is

$$\gamma(\mathcal{P}, \mathcal{P}_s) \doteq \max_{a \in \mathcal{A}} |J(\xi, a) - J_s(\xi_s, a)|. \quad (4)$$

The *balanced simplification offset* between the problems is

$$\gamma^*(\mathcal{P}, \mathcal{P}_s) \doteq \min \{ \gamma(\mathcal{P}, \mathcal{P}_s^f) \mid f: \mathbb{R} \rightarrow \mathbb{R} \text{ is monotonically increasing} \wedge \mathcal{P}_s^f \doteq (\xi_s, \mathcal{A}, f \circ J_s) \}. \quad (5)$$

The offset measures the maximal difference between respective objective values of two problems. Furthermore, according to Theorem 1, every monotonically increasing

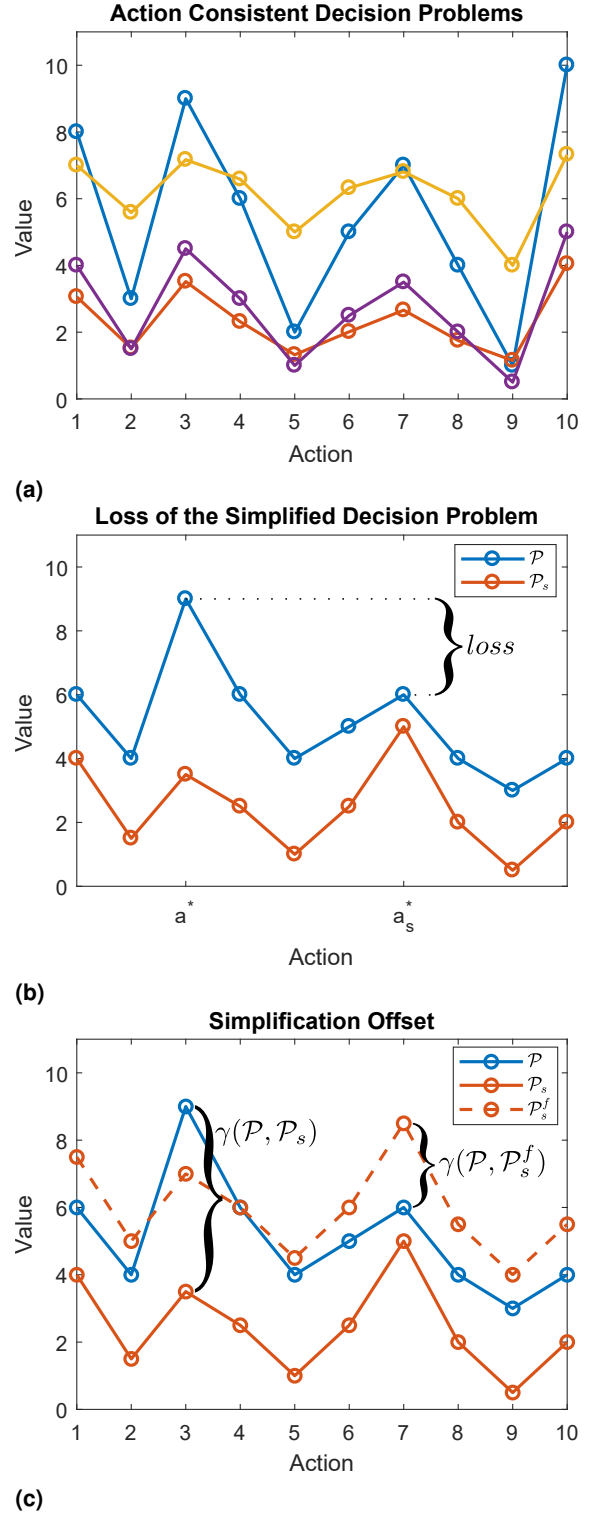


Figure 1. (a) Conceptual demonstration of *action consistency*: each graph represents the objective function values of the candidate actions, for some decision problem; although the values are different, all the graphs maintain the same trend among the actions, and therefore are action consistent. (b) Conceptual demonstration of the *loss*: \mathcal{P}_s is a simplification of a decision problem \mathcal{P} ; a_s^* is the optimal action according to the simplified problem, and a^* is the real optimal action; the difference between the (real) objective function values of these two actions is the loss induced by the simplification. (c) Conceptual demonstration of the *simplification offset*: the offset between \mathcal{P} and \mathcal{P}_s is the maximal difference between the values of *respective* actions; the offset can be reduced by applying a balance function f (here we used a constant-shift).

balance function f can be used to define a decision problem \mathcal{P}_s^f which is action consistent with \mathcal{P}_s . Hence, the balanced offset is the minimal offset between \mathcal{P} and any problem action consistent with \mathcal{P}_s . A demonstrative example appears in Fig. 1c. Specifically, if $\mathcal{P} \simeq \mathcal{P}_s$, then the balanced offset is zero. This is also a sufficient condition for action consistency.

Corollary 2.

$$\mathcal{P} \simeq \mathcal{P}_s \iff \gamma^*(\mathcal{P}, \mathcal{P}_s) = 0. \quad (6)$$

The balanced offset scales the simplified objective values according to the original ones, and therefore is not a symmetric distance. Fittingly, this property matches the loss, which is also asymmetric. The balanced offset does, however, comply to the triangle inequality.

Theorem 2.

The balanced offset complies to the triangle inequality:

$$\gamma^*(\mathcal{P}_1, \mathcal{P}_2) + \gamma^*(\mathcal{P}_2, \mathcal{P}_3) \geq \gamma^*(\mathcal{P}_1, \mathcal{P}_3). \quad (7)$$

These properties, along with the obvious non-negativity, make the balanced offset a quasi-metric (or asymmetric metric), which induces an appropriate topology on the space of decision problems, as explained by Künzi (2001).

2.4 Guarantees

Generally, the exact loss is unknown without solving the original problem; yet, using the solution of the simplified problem, it can be bounded. We should point out that bounding the loss is not required in order to take advantage of the concept of problem simplification. Rather, it is an analytic tool which allows to guarantee the quality of solution. As to be seen, even without proving tight bounds, a smartly simplified problem can still induce minimal or zero loss, in practice. Guarantees can be calculated offline, as post-processing, or online, before solving the problem, to help deciding whether the simplification is good enough to use, under some accuracy requirement. Such requirement can be given as a threshold over the maximal loss. This can be the case when action execution (as measured with the objective function) is costly, and beyond a certain loss, improving the decision making efficiency is not worth the execution of sub-optimal action. In this case we would rather invest in a more accurate action selection, in order to find a less costly action. We can derive a loss bound directly from its definition:

$$\text{loss}(\mathcal{P}, \mathcal{P}_s) \leq \text{UB} \{J(\xi, a^*)\} - \text{LB} \{J(\xi, a_s^*)\} \leq \max_{a \in \mathcal{A}} \text{UB} \{J(\xi, a)\} - \text{LB} \{J(\xi, a_s^*)\}, \quad (8)$$

where UB, LB stand for upper and lower bounds, respectively. These bounds on the objective function should be selected in the context of the problem; we demonstrate how to do so in Section 3.2.4. If the examined simplification is known to always over/underestimate the original objective values, this expression can be tightened. When $J(\xi, a) \geq J_s(\xi_s, a), \forall a \in \mathcal{A}$,

$$\text{loss}(\mathcal{P}, \mathcal{P}_s) \leq \max_{a \in \mathcal{A}} \text{UB} \{J(\xi, a)\} - J_s(\xi_s, a_s^*), \quad (9)$$

and when $J(\xi, a) \leq J_s(\xi_s, a), \forall a \in \mathcal{A}$,

$$\text{loss}(\mathcal{P}, \mathcal{P}_s) \leq J_s(\xi_s, a_s^*) - \text{LB} \{J(\xi, a_s^*)\}. \quad (10)$$

The quality of the aforementioned loss bounds depends directly and solely on the tightness of UB and LB . Alternatively and intuitively, the simplification offset can also be used to bound the loss. Theorem 3 indicates that when the (balanced) offset between a problem and its simplification is small, then the induced loss is also small, and the action selection stays “similar”.

Theorem 3.

$$0 \leq \text{loss}(\mathcal{P}, \mathcal{P}_s) \leq 2 \cdot \gamma^*(\mathcal{P}, \mathcal{P}_s). \quad (11)$$

We recognize that the balanced offset is also unknown without solving the original problem; therefore, in practice, we use a bound over it to bound the loss. We recall that for *any* monotonically increasing balance function f , $\gamma^*(\mathcal{P}, \mathcal{P}_s) \leq \gamma(\mathcal{P}, \mathcal{P}_s^f)$. Also, the offset notably measures the difference between the original and simplified objective values for *the same* action (unlike the loss); in certain problems, this property can be exploited to derive a custom bound over the offset, which would lead to a tighter loss bound, without relying on UB and LB . We demonstrate this idea in a practical scenario in Section 3.2.4, but, for the sake of intuition, let us examine this simple example:

Consider decision problems $\mathcal{P} = (x, \mathcal{A}, \cdot), \mathcal{P}_s = (x_s, \mathcal{A}, \cdot)$, where $x, x_s \in \mathbb{R}, \mathcal{A} \subset \mathbb{R}$, the objective function is a multiplication between the inputs, and f is a scaling function by a factor of c . Then, $\gamma^*(\mathcal{P}, \mathcal{P}_s) \leq \gamma(\mathcal{P}, \mathcal{P}_s^f) = \max_a |(x \cdot a) - c \cdot (x_s \cdot a)| = |x - c \cdot x_s| \cdot \max_a |a|$. Thus, in this case, we are able to separate the “influence” of the simplification process from the examined action. Furthermore, by changing the selection of f , we are able to adjust the tightness of this bound.

3 Efficient Belief Space Planning

In the previous section we introduced a new concept for the efficient solution of decision problems – identifying a simplified analogous problem, and solving it instead. Now we wish to apply this idea to decision making under uncertainty, and discuss BSP problems. In this case, the initial state of the decision problem is actually the prior belief, and, as to be explained, the problem is simplified by considering a sparse approximation of it. We provide an appropriate sparsification algorithm, and then show that the induced loss can be bounded. First of all, we define the BSP problem.

3.1 Problem Definition

We consider a sequential BSP scenario, under a POMDP framework. At time-step k , the agent transitions from pose x_{k-1} to pose x_k , using a control u_k . It then receives an observation of the world z_k , based on this updated state. The transition and observation are both probabilistic operations. At each time-step, the agent maintains the posterior distribution over its state current vector \mathbf{X}_k , given the controls and observations until that time; this distribution is also known as its *belief*:

$$b_k \doteq \mathbb{P}(\mathbf{X}_k \mid u_{1:k}, z_{1:k}), \quad (12)$$

where $u_{1:k} \doteq \{u_1, \dots, u_k\}$ and $z_{1:k} \doteq \{z_1, \dots, z_k\}$. The agent’s state vector consists of the series of poses, and may

also include external variables, which are introduced by the observations, i.e. $\mathbf{X}_k \doteq (\mathbf{x}_0^T, \dots, \mathbf{x}_k^T, \mathbf{L}_k^T)^T$. For example, in a full-SLAM scenario, \mathbf{L}_k can stand for the positions of maintained landmarks. Please note, we only describe the process as sequential for generalization; our approach considers every planning session as a separate problem. Also, in order not to force any marginalization of past poses, we optimize the entire trajectory of poses, i.e. a smoothing paradigm. Both assumptions are not essential to our approach.

We assume the belief b_k is normally-distributed. Hence, to describe it, we can use the covariance matrix Σ_k , or equivalently the (Fisher) information matrix Λ_k ; these matrices are each other's inverse:

$$b_k = \mathcal{N}(\hat{\mathbf{X}}_k, \Sigma_k) \equiv \mathcal{N}(\hat{\mathbf{X}}_k, \Lambda_k^{-1}). \quad (13)$$

The transition and observation models are described with the following dependencies:

$$\mathbf{x}_k = g_k(\mathbf{x}_{k-1}, \mathbf{u}_k) + \mathbf{w}_k, \quad \mathbf{w}_k \sim \mathcal{N}(0, \mathbf{W}_k), \quad (14)$$

$$\mathbf{z}_k = h_k(\mathbf{X}_k) + \mathbf{v}_k, \quad \mathbf{v}_k \sim \mathcal{N}(0, \mathbf{V}_k), \quad (15)$$

where $\mathbf{W}_k, \mathbf{V}_k$ are the covariance matrices of the respective normally-distributed zero-mean noise models $\mathbf{w}_k, \mathbf{v}_k$, and g_k, h_k are deterministic functions. We can now reason about an updated belief at time $k+1$, after performing a control \mathbf{u}_{k+1} and taking an observation \mathbf{z}_{k+1} :

$$b_{k+1} \doteq \mathbb{P}(\mathbf{X}_{k+1} \mid \mathbf{u}_{1:k+1}, \mathbf{z}_{1:k+1}) \propto b_k \cdot \mathbb{P}(\mathbf{x}_{k+1} \mid \mathbf{x}_k, \mathbf{u}_{k+1}) \cdot \mathbb{P}(\mathbf{z}_{k+1} \mid \mathbf{X}_{k+1}). \quad (16)$$

From here, a simple update rule for the information matrix can be derived, such that

$$\Lambda_{k+1} = \check{\Lambda}_k + \mathbf{G}_{k+1}^T \mathbf{W}_{k+1}^{-1} \mathbf{G}_{k+1} + \mathbf{H}_{k+1}^T \mathbf{V}_{k+1}^{-1} \mathbf{H}_{k+1}, \quad (17)$$

where the matrices \mathbf{G}_{k+1} and \mathbf{H}_{k+1} are the Jacobians $\nabla g_{k+1}|_{\bar{\mathbf{x}}_{k+1}}$ and $\nabla h_{k+1}|_{\bar{\mathbf{x}}_{k+1}}$, respectively, around some initial estimate, and $\check{\Lambda}_k$ is the augmented prior information matrix (for a full derivation see, e.g., Indelman et al. (2015)).

As controls and observations may introduce new variables to the state vector, its size at time-step k , often does not match its size at time-step $k+1$. Hence, the prior information matrix Λ_k should be augmented to accommodate these new variables. We use the accent $\check{}$ to indicate augmentation of the prior information matrix (with entries of zero) to match the posterior size. Adding new variables is possible at any index in the state, as long as we make sure the augmentation keeps the same variable order. If the prior state is of size n , and we add m new variables to the end of it, then

$$\check{\Lambda}_k \doteq \left(\begin{array}{c|c} \Lambda_k^{n \times n} & \mathbf{0}^{n \times m} \\ \hline \mathbf{0}^{m \times n} & \mathbf{0}^{m \times m} \end{array} \right). \quad (18)$$

The expression in Eq. 17 can be written in a more compact form, using the *collective Jacobian* \mathbf{U}_{k+1} , which encapsulates the new information regarding the control and the succeeding observation:

$$\Lambda_{k+1} = \check{\Lambda}_k + \mathbf{U}_{k+1}^T \mathbf{U}_{k+1}, \quad \text{where } \mathbf{U}_{k+1} = \begin{bmatrix} \mathbf{W}_{k+1}^{-\frac{1}{2}} \mathbf{G}_{k+1} \\ \mathbf{V}_{k+1}^{-\frac{1}{2}} \mathbf{H}_{k+1} \end{bmatrix}. \quad (19)$$

Each control can be described using a collective Jacobian of this form. Thanks to the additivity of the information, we can easily examine the information matrix after applying a sequence of T controls $u \doteq u_{k+1:k+T}$; the respective collective Jacobians of each control can simply be stacked to yield the collective Jacobian \mathbf{U} of the entire sequence:

$$\Lambda_{k+T} = \check{\Lambda}_k + \sum_{t=1}^T \mathbf{U}_{k+t}^T \mathbf{U}_{k+t} = \check{\Lambda}_k + \mathbf{U}^T \mathbf{U}, \quad \text{where } \mathbf{U} \doteq \begin{bmatrix} \mathbf{U}_{k+1} \\ \vdots \\ \mathbf{U}_{k+T} \end{bmatrix}. \quad (20)$$

Now, considering a set \mathcal{U} of such candidate control sequences, we wish to select the one which minimizes the expected uncertainty in the future belief. To measure the uncertainty we use the (differential) entropy, which, for a normally-distributed belief b , over a state of size N , with an information matrix Λ , is

$$\mathbb{H}(b) = \frac{1}{2} \cdot \ln \left[\frac{(2\pi e)^N}{|\Lambda|} \right] = -\frac{1}{2} \cdot (\ln|\Lambda| - N \cdot \ln(2\pi e)). \quad (21)$$

Thus, while utilizing the information update rule from Eq. 20, we can define the following objective function for this decision problem:

$$J(b_k, u) \doteq \mathbb{E}_{\mathcal{Z}} [-\mathbb{H}(b_{k+T})] = \frac{1}{2} \cdot \mathbb{E}_{\mathcal{Z}} \left[\ln|\check{\Lambda}_k + \mathbf{U}^T \mathbf{U}| - N \cdot \ln(2\pi e) \right], \quad (22)$$

where u is a candidate control sequence with a collective Jacobian \mathbf{U} , \mathcal{Z} is the set of observations taken while performing this sequence, and N is the posterior state size (the number of columns in \mathbf{U}). To be able to drop the expectation, we take the very common assumption of achieving the most likely observations, around the current mean (“maximum likelihood” assumption (Platt et al. 2010)). We also drop the augmentation mark and time index from now on, for the sake of concise writing. Thus, we can conclude the final form of the objective function,

$$J(b, u) = \frac{1}{2} \cdot (\ln|\Lambda + \mathbf{U}^T \mathbf{U}| - N \cdot \ln(2\pi e)), \quad (23)$$

where Λ is the information matrix of the prior belief b , and \mathbf{U} is the collective Jacobian of u . Certainly the determinant of the posterior information matrix $\Lambda + \mathbf{U}^T \mathbf{U}$ is non-negative (positive semi-definite matrix), and larger than this of the prior (as explained in Eq. 40); however, the objective function may still yield values which are negative, or lower than the “prior value”, due to the normalization element.

For clarification, the “maximum likelihood” assumption is not essential in order to apply our method, but is used to achieve a clear discussion, where each candidate control sequence can be described using a single collective Jacobian. Also, using the information form to examine the future beliefs can be done even if the state inference process is not based on such information smoother/filter. If the current information matrix is not provided through state inference, it can be calculated by inverting the covariance matrix. This inversion would be done once for each decision, with no relation to the number of candidates.

3.1.1 Alternative Formulation: Information Root Matrix

An alternative way to represent the belief is using the upper triangular square root \mathbf{R}_k of the information matrix $\mathbf{\Lambda}_k$, given (e.g.) by the Cholesky decomposition:

$$\mathbf{\Lambda}_k = \mathbf{R}_k^T \mathbf{R}_k. \quad (24)$$

This representation is used, while exploiting inherent sparsity, in prominent state-of-the-art SLAM algorithms, such as iSAM2 (Kaess et al. 2012). In this form, the determinant of the information can be calculated in linear time – using the multiplication of the diagonal elements of the triangular matrix; on the other hand, the information update loses its convenient additivity property, and requires re-calculation (or update) of the factorization, in order to find the posterior triangular root matrix \mathbf{R}_{k+T} , such that

$$\mathbf{R}_{k+T}^T \mathbf{R}_{k+T} = \mathbf{\Lambda}_{k+T} = \begin{pmatrix} \check{\mathbf{R}}_k \\ \mathbf{U} \end{pmatrix}^T \begin{pmatrix} \check{\mathbf{R}}_k \\ \mathbf{U} \end{pmatrix}, \quad (25)$$

where \mathbf{U} is defined as in Eq. 20. Using this form, the significant computational cost of calculating the objective function (Eq. 23) moves from the determinant calculation to the information update phase. To match the previous notation, $\check{\mathbf{R}}_k$ is an augmentation of the prior root matrix

$$\check{\mathbf{R}}_k \doteq \left(\mathbf{R}_k^{n \times n} \mid \mathbf{0}^{n \times m} \right), \quad (26)$$

As explained, new variables can be added to the state at any index. The augmentation is indicated here at the end of the state for convenience.

3.2 Sparse Belief Approximations

We now wish to present a simplification method for the decision problem we have just formalized: $\mathcal{P} \doteq (b, \mathcal{U}, J)$. Here, we keep the same objective function J (as defined in Eq. 23), and set \mathcal{U} of candidate actions, and focus on simplifying the initial belief b . As stated, candidate actions here are actually control sequences for the agent; we assume the collective Jacobians for the set of actions are available.

As we saw, in BSP, calculation of the objective function involves calculation of the determinant of the posterior information matrix (Eq. 23). The cost of this calculation depends directly on the number of non-zero elements in the matrix, and is significantly lower for sparse matrices. Thus, sparsifying the posterior information matrices shall reduce the cost of solving the problem, as desired. Thanks to the additivity of the information, sparsifying the prior information matrix $\mathbf{\Lambda}$ essentially leads to sparser posterior information matrix $\mathbf{\Lambda} + \mathbf{U}^T \mathbf{U}$, for every candidate action u with collective Jacobian \mathbf{U} . Notably such sparsification of the prior is only calculated once, for any number of actions. We also note that in many problems, especially in navigation problems, the collective Jacobians are also sparse, and over time, as the state grows, involve less variables in relation to the state size. Hence, even after adding the new information, the posterior information matrix shall remain sparse. Overall, assuming the initial belief of a certain BSP problem is $b = \mathcal{N}(\mathbf{X}, \mathbf{\Lambda}^{-1})$, the simplified problem shall rely instead on $b_s = \mathcal{N}(\mathbf{X}, \mathbf{\Lambda}_s^{-1})$ as the initial belief, where $\mathbf{\Lambda}_s$ is a

sparse approximation of $\mathbf{\Lambda}$. Equivalently, if discussing the alternative information root formulation, we seek to sparsify \mathbf{R} , the square root of the prior information matrix, in order to improve the factorization update process.

In the following section we specify a sparsification algorithm for the information matrix (or its square root matrix). Fig. 2 summarizes the paradigm of belief sparsification for the efficient solution of BSP problems; clarification regarding the optional steps which appear in the chart is to follow.

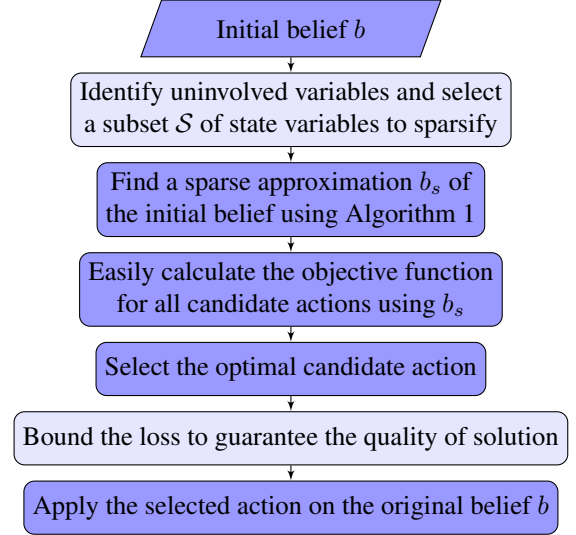


Figure 2. Using belief sparsification for the efficient solution of BSP problems. Essential steps are in dark blue, and optional steps are in light blue. Here, candidate actions represent control sequences for the agent.

3.2.1 The Algorithm Algorithm 1 summarizes our suggested method for sparsification of a given belief. The algorithm may receive as input, and return as output, either the information matrix of the belief, or its triangular square root. This scalable algorithm depends on a pre-selected subset \mathcal{S} of state variables, and wisely removes elements which correspond to these variables from the matrix. Approximations of different degrees can be generated using different variable selections \mathcal{S} , as to be explained in Section 3.2.3. For a clear discussion, when \mathcal{S} contains all the variables, we say this is a *full sparsification*; using any other partial selection of variables is a *partial sparsification*.

Essentially, the algorithm removes off-diagonal elements from the given belief’s information root matrix, in rows corresponding to the sparsified variables in \mathcal{S} , as long as these variables appear first in the state. Hence, when given the information matrix (and not its root), and/or the variable order is not the desired one, the input should initially be brought to the desired sparsifiable form.

Let us break down the algorithm steps: First (line 1), we check if the variables are ordered properly, i.e. such that the variables we wish to sparsify (variables in \mathcal{S}) appear first in the state. If not, we should reorder the variables accordingly. If the algorithm input is the information root matrix \mathbf{R} (line 2), we should resort to the symmetric information matrix $\mathbf{\Lambda}$, as trying to permute the variables in the root directly would break its triangular shape. Thus, if needed, in line 3, we reform the information matrix from its root,

Algorithm 1: Scalable Belief Sparsification

Inputs:

- └ A belief $b = \mathcal{N}(\mathbf{X}, \Lambda^{-1})$, s.t. $\Lambda = \mathbf{R}^T \mathbf{R}$
- └ A subset \mathcal{S} of state variables to sparsify

Output:

- └ A sparsified belief b_s

- 1 **if** the variables in \mathcal{S} are **not** first in the variable order **then**
- 2 **if** the algorithm input is \mathbf{R} **then**
- 3 └ Form the information matrix $\Lambda \doteq \mathbf{R}^T \mathbf{R}$
- 4 Permute the variables in Λ s.t. the variables in \mathcal{S} are first in the variable order
- 5 └ Calculate $\mathbf{R} \doteq \text{chol}(\Lambda)$
- 6 **else if** the algorithm input is Λ **then**
- 7 └ Calculate $\mathbf{R} \doteq \text{chol}(\Lambda)$
- 8 Remove off-diagonal elements from \mathbf{R} in rows matching variables in \mathcal{S} , to create \mathbf{R}_s
- 9 Permute the variables in \mathbf{R}_s back to their original order
- 10 **return** $b_s \doteq \mathcal{N}(\mathbf{X}, \Lambda_s^{-1})$, s.t. $\Lambda_s \doteq \mathbf{R}_s^T \mathbf{R}_s$

before permuting the variables (line 4). This permutation is required in order to minimize fill-in, and to properly decorrolate the sparsified variables from the unsparsified ones – a requirement in the proof of Theorem 4, which is to appear in the next section, and which provides certain guarantees for the approximated belief. Such permutation is done by calculating the product $\mathbf{P}\Lambda\mathbf{P}^T$ of the information matrix with an appropriate permutation matrix \mathbf{P} .

After the permutation, we calculate the square root matrix of the permuted information matrix, using the Cholesky decomposition (line 5). If no reordering is required, and the algorithm input is the information matrix Λ (line 6), we may directly calculate the Cholesky decomposition (line 7); if no reordering is required, and the input is the root \mathbf{R} , we may skip directly to line 8. Specifically, when all of \mathcal{S} is already at the beginning of the state, no reordering is needed. This situation particularly occurs with a full sparsification, i.e. when sparsifying *all* the variables.

Next, in line 8 we zero off-diagonal elements in the (permuted) root matrix, in the rows corresponding to variables in \mathcal{S} , resulting in the sparsified root matrix \mathbf{R}_s .

Finally, we reorder the variables back to their original order (line 9). Though, we notice that after the sparsification this permutation can actually be done *in the root form* directly, without resorting to the information matrix, and without breaking the triangular shape, by calculating $\mathbf{P}^T \mathbf{R}_s \mathbf{P}$ (same permutation matrix used before; note the reverse multiplication order); this claim is given in Corollary 3. Alternatively, the permutation of variables back to their original order can be skipped, by instead permuting the columns of all the candidate collective Jacobians, to match the altered order.

Corollary 3.

After sparsification of the information root matrix (line 8 of Algorithm 1), permuting the variables back to their original order can be performed in the information root matrix directly, without breaking its triangular shape.

In line 10, we return the sparsified belief, represented either via \mathbf{R}_s or Λ_s . In the latter case, this line holds an implicit cost of reforming the information matrix from

its root. With a full sparsification, \mathbf{R}_s and hence Λ_s are diagonal, giving linear complexity to both the final variable reordering, and the reformation of the information. Also, permutation of the symmetric information matrix is relatively negligible. The decomposition (when conducted) is the costliest step of the algorithm – the complexity of the Cholesky decomposition is $O(N^3)$, at worst, where N is the state size (Hämmerlin and Hoffmann 2012). As explained, when the input information root matrix is already in the desired order, the permutation and decomposition steps can be skipped, giving the algorithm an almost negligible complexity. Since full sparsification leads to a diagonal approximation (information or its root), considering the collective Jacobians are sparse, we get almost linear complexity for the objective function calculation. Thus, this method allows us to enjoy the benefits of a high quality information measure (entropy), at the computational cost of a simple information measure (such as trace), while experiencing minimal loss, as to be seen.

Fig. 3 shows a comparison of a given information root matrix and its sparse approximations generated with Algorithm 1, for different variable selections \mathcal{S} : partial sparsification (about half of the variables), and full sparsification.

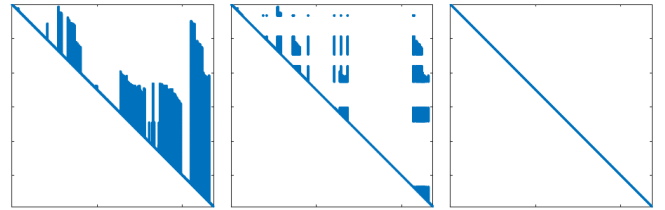


Figure 3. Comparison of a given information root matrix and its sparse approximations generated with Algorithm 1, for different variable selections \mathcal{S} . On the left – the original matrix; in the center – the matrix after partial sparsification of about half of the variables; on the right – the matrix after full sparsification. Information regarding each sparsified variable is represented with a diagonal entry; information regarding the remaining variables is updated due to correlations. A full sparsification results in a convenient diagonal approximation of the information. For all degrees of sparsification, the determinant of the matrix remains the same.

Remark Currently, in Algorithm 1 we consider a full re-factorization of the square root matrix, in order to permute the variables. We are aware that the cost of this step can possibly be lowered, using a partial/incremental factorization, as done today in the context of state inference (e.g. iSAM2 by Kaess et al. (2012)). This improvement to the algorithm will be examined in our future work.

3.2.2 Probabilistic Insights Off-diagonal entries in the triangular information root matrix indicate conditional dependency between variables. Such entries in the information matrix indicate direct links (factors) between variables, e.g. those created by a multi-variate observation or constraints between poses. Variables can be conditionally dependent even if there is no direct link between them (and this is why the root matrix is denser than the information matrix). Practically, fixing a certain order of the state variables corresponds

to a specific decomposition of the belief to a product of conditional probabilities; a variable may only be dependent on a variable with a higher index. Hence, the initial reordering of the variables signifies conditional separation of the variables for sparsification \mathcal{S} and the remaining variables $\neg\mathcal{S}$, s.t

$$b \doteq \mathbb{P}(\mathbf{X}) = \mathbb{P}(\mathcal{S} \mid \neg\mathcal{S}) \cdot \mathbb{P}(\neg\mathcal{S}). \quad (27)$$

Since the algorithm removes the off-diagonal entries in rows corresponding the sparsified variables in the root matrix, it essentially removes their dependencies. The conditional probability over the sparsified variables thus turns into a product of independent marginals

$$b \approx \prod_{i=1}^{|\mathcal{S}|} \mathbb{P}(S_i) \cdot \mathbb{P}(\neg\mathcal{S}). \quad (28)$$

The initial variable reordering makes sure the inner dependencies among the non-sparsified variables remain exact, and will later allow us to develop performance guarantees (Theorem 4). When updating this approximated belief, for example, when a new observation involving an existing variable arrives (i.e. loop closure), information would no longer propagate from a sparsified variable to another variable, or vice versa, unless they are both observed together.

Notably, the algorithm works on the underlying Bayesian network, which is analogous to the information root matrix; removing entries from the matrix corresponds to removing edges from the network, which in turn corresponds to removing conditional dependencies. On the contrary, traditional belief sparsification methods (as previously reviewed) perform sparsification on the information matrix, or equivalently, the factor graph. In the information domain, the influence of sparsification, i.e. removal of graph edges/matrix entries, over the belief is not as straight forward. After performing our suggested algorithm, entries in the information matrix may change, and new factors between non-sparsified variables may be added in compensation for the removed correlations, in a similar way to marginalization. This update to the factors is performed implicitly by manipulating the root matrix. Specifically, the diagonal of the sparsified information matrix and the original one are not identical. Unlike marginalization, however, sparsified variables are not “deleted” from the state, and they can still be updated.

Moreover, as our sparsification does not change the eigenvalues of the distribution (diagonal entries in the information root matrix), it does not change the base entropy of the system. Meaning, the determinants of $\mathbf{\Lambda}$ and $\mathbf{\Lambda}_s$ remain the same, no matter which variables are sparsified (Eq. 66 in Appendix A). This is usually not guaranteed in the aforementioned traditional sparsification methods. Divergence in entropy between the exact and approximated beliefs might only happen after applying a new action, depending on the variable selection, as to be discussed.

3.2.3 Variable Selection Considering a specific action, a state variable is *involved* if applying the action directly impacts the variable; i.e., if g or h , which define the relevant transition and observation models (Eq. 14-15), are a function of this variable. Practically, in the collective Jacobian of an

action, each of the columns represents a variable in the state vector; a variable is involved if at least one of the entries in its matching column is non-zero; uninvolved variables correspond to columns of zeros. In a navigation scenario, for example, the observed landmarks and current pose are *involved*; variables referring to landmarks from the past, which are not be observed anymore, are *uninvolved*. In this scenario, after a while, most landmarks are expected to be out of the visible range, and only a small portion of nearby landmarks shall remain relevant.

We claim that sparsification of uninvolved variables does not affect the posterior information determinant. Hence, when sparsifying variables which are uninvolved for all the actions, the objective function values are unaffected, and the resulting approximation is action consistent. This claim is expressed in Theorem 4; its proof is given in Appendix A. We emphasize that since this is a planning problem, we *know* what the involved variables are, given the set of action. There is no risk that unexpected loop closures would occur, as might happen in state inference.

Theorem 4.

Consider a belief b , a set of candidate actions \mathcal{U} , and the objective function J (from Eq. 23). For a set \mathcal{S} of variables, which are uninvolved for the entire set of actions \mathcal{U} , Algorithm 1 returns a belief b_s s.t. $J(b, u) = J(b_s, u)$, $\forall u \in \mathcal{U}$. Specifically, $b \simeq b_s$.

In principle, only a single sparsification process is conducted for each decision problem (i.e. planning session), regardless of the number of candidate actions. Selecting variables which are uninvolved for all the candidate actions allows to keep action consistency considering the entire set of candidates. Still, it is possible to break to set of actions to several subsets of similar actions, and consider the uninvolved variables in each subset. For each subset we would create a custom prior approximation, and then select the best candidate in each of the subsets, before finding the overall best candidate among those. This can result in a more adapted sparsification for each subset. Yet, calculation of the sparsification itself has a cost, which needs to be considered when trying to achieve the best performance. Here we examine the most general case – treating the set of actions as a whole.

We proved that sparsifying uninvolved variables does not affect the objective function values, and therefore they should always be included in the set \mathcal{S} of variables for sparsification. It is possible to sparsify also involved variables, but then action consistency is not guaranteed. For example, if we do not consider major loop closures (and most existing variables are uninvolved), we might decide to perform full sparsification. Intuitively, selecting more variables to \mathcal{S} results in a sparser approximation, and also a larger divergence from the original objective values.

As discussed in Section 2.4, assuming it is possible to tolerate a certain degree of inaccuracy in the results (a “budget”), we can use the loss bound to analyze whether using a certain sparsification guarantees not to exceed this allowance, before actually performing the decision making. Finding the optimal (involved) variable selection for the sparsification, under the accuracy constraints, is by itself an

optimization problem. We aspire to select the most cost-effective set S , that gives the highest degree of sparsification under this budget. This can be done by scalably enlarging S according to some heuristic, until the bound no longer guarantees satisfying results. Other options are random selections until the criteria is met, genetic algorithms, etc. While a wise selection of S also bares a certain cost, it can prove itself profitable, especially for a large set of candidate actions, where the initial investment becomes less significant. Nonetheless, in the results to follow, we demonstrate that even when sparsifying all the variables, the quality of solution is still well preserved.

3.2.4 Guarantees Consider the problem $\mathcal{P} \doteq (b, \mathcal{U}, J)$, and its simplification $\mathcal{P}_s \doteq (b_s, \mathcal{U}, J)$ – using a sparse approximation of the initial belief. As mentioned, it is indeed possible to select also involved variables for sparsification, but in this case action consistency is not guaranteed, and divergence between the real and approximated action values might occur. This divergence is measured using the $loss(\mathcal{P}, \mathcal{P}_s)$, as explained in Section 2.1. In the following discussion we demonstrate how to bound the loss between the original decision problem, and the one which uses a sparse belief approximation, created with Algorithm 1 for a given set S . First, we show that when certain conditions are known, we can derive such loss by bounding the simplification offset (Definition 4); we then examine a more general case, in which we bound the loss directly.

Rank-1 Updates Assume that for every action $u \in \mathcal{U}$ the corresponding collective Jacobian $U \in \mathbb{R}^{1 \times N}$ contains only a single row, i.e. rank-1 information updates. This can be the case, for example, in sensor placement problems with scalar measurements (like temperature). According to Theorem 3 in Section 2.4, we can use (a bound of) the offset between the problem and its simplification, to derive a loss bound. We also mentioned that for certain decision problems, the offset can be bounded without having to explicitly calculate the objective values. Let us demonstrate so here:

$$|J(b, u) - J(b_s, u)| = \quad (29)$$

$$|\ln|\Lambda + U^T U| - \ln|\Lambda_s + U^T U|| = \quad (30)$$

(Matrix determinant lemma (see Harville 1998))

$$|\ln(|\Lambda| \cdot (1 + U\Lambda U^T)) - \ln(|\Lambda_s| \cdot (1 + U\Lambda_s U^T))| = \quad (31)$$

(Eq. 66)

$$|\ln(1 + U\Lambda U^T) - \ln(1 + U\Lambda_s U^T)| = \quad (32)$$

$$|\ln(1 + U\Lambda_s U^T + U(\Lambda - \Lambda_s)U^T) - \ln(1 + U\Lambda_s U^T)| \leq \quad (33)$$

(★)

$$|\ln(1 + U(\Lambda - \Lambda_s)U^T) - \ln(1)| = \quad (34)$$

$$|\ln(1 + U(\Lambda - \Lambda_s)U^T)| \leq \quad (35)$$

$$\left| \ln \left(1 + \alpha \cdot \sum_{i,j \in \mathcal{I}nv(u)} (\Lambda - \Lambda_s)_{ij} \right) \right|, \quad (36)$$

where $\mathcal{I}nv(u)$ is the set of variables involved in u , and the scalar α complies to $\alpha \geq \max_i U_i^2$. We recall that U_i is uninvolved $\iff U_i = 0$. When considering the involved

variables among all the actions, and α is valid $\forall u \in \mathcal{U}$, this bound becomes independent of a specific action, and only a single expression needs to be calculated. Overall we can conclude the following bound on the (balanced) offset:

$$\gamma^*(\mathcal{P}, \mathcal{P}_s) \leq \left| \ln \left(1 + \alpha \cdot \sum_{i,j \in \mathcal{I}nv(\mathcal{U})} (\Lambda - \Lambda_s)_{ij} \right) \right|. \quad (37)$$

(★) According to the Minkowski determinant inequality and the matrix determinant lemma, $|\Lambda_s| \leq |\Lambda_s + U^T U| = |\Lambda_s| \cdot (1 + U\Lambda_s U^T)$ thus $0 \leq U\Lambda_s U^T$. Now, since the logarithm is a monotonously increasing concave function, the transition is correct.

General Case For a more general scenario, with actions possibly having multi-row collective Jacobians, representing non-myopic actions, we can use the loss bound from Eq 8. In this general expression, we should only assign upper and lower bounds of the objective function ($\mathcal{UB}, \mathcal{LB}$, respectively). We provide several options for such bounds. It is possible to use various other options in a similar manner.

Using Determinant Bounds First, we use known determinant bounds. For the lower bound, we can use the *Minkowski determinant inequality*, which states that for positive semi-definite matrices $M_1, M_2 \in \mathbb{R}^{N \times N}$

$$|M_1 + M_2|^{\frac{1}{N}} \geq |M_1|^{\frac{1}{N}} + |M_2|^{\frac{1}{N}}, \quad (38)$$

$$\ln|M_1 + M_2| \geq N \cdot \ln \left(|M_1|^{\frac{1}{N}} + |M_2|^{\frac{1}{N}} \right). \quad (39)$$

Let us assign $M_1 \doteq \Lambda$, $M_2 \doteq U^T U$; when $U^T U$ is not a full rank update (e.g. U has less than N rows), $|U^T U| = 0$, and we are left with

$$\ln|\Lambda + U^T U| \geq \ln|\Lambda| \quad (40)$$

For formality, it is easy to show that even if the prior state size is smaller than N , the validity of the conclusion is not compromised (in a similar way to Eq. 69). For the upper bound, we can use the *Hadamard inequality*, which states that for a positive semi-definite matrix $M \in \mathbb{R}^{N \times N}$

$$|M| \leq \prod_{i=1}^N (M)_{ii}. \quad (41)$$

Let us assign $M \doteq \Lambda + U^T U$; then

$$|\Lambda + U^T U| \leq \prod_{i=1}^N (\Lambda + U^T U)_{ii}, \quad (42)$$

$$\ln|\Lambda + U^T U| \leq \sum_{i=1}^n \ln[(\Lambda + U^T U)_{ii}]. \quad (43)$$

Overall, we get the following bounds for the objective function:

$$\mathcal{LB}_{\det} \{J(b, u)\} \doteq \ln|\Lambda| - N \cdot \ln(2\pi e), \quad (44)$$

$$\mathcal{UB}_{\det} \{J(b, u)\} \doteq \sum_{i=1}^N \ln[(\Lambda + U^T U)_{ii}] - N \cdot \ln(2\pi e), \quad (45)$$

where Λ is the information matrix of prior belief b , and $U \in \mathbb{R}^{m \times N}$ is the collective Jacobian of action u .

Using Topological Bounds When BSP problems are represented with (factor) graphs, we can also exploit topological properties of the beliefs. For example, in recent works (Khosoussi et al. 2018; Kitanov and Indelman 2019), the following bounds on the entropy of a belief were proved, for when the corresponding factor graph contains only the agent’s poses, and each pose consists of the position and the orientation of the agent (i.e. pose-SLAM):

$$\mathcal{LB}_{\text{top}} \{J(b, u)\} \doteq 3 \cdot \tau(b, u) + \mu, \quad (46)$$

$$\mathcal{UB}_{\text{top}} \{J(b, u)\} \doteq$$

$$\mathcal{LB}_{\text{top}} \{J(b, u)\} + \sum_{i=2}^n \ln(d_i + \Psi) - \ln|\tilde{\mathbf{L}}|, \quad (47)$$

where $\tau(b, u)$ stands for the number of spanning trees in the factor graph of the posterior belief (b after applying u); $\tilde{\mathbf{L}}$ is the reduced Laplacian matrix of this graph; and d_i ’s are the node degrees corresponding to $\tilde{\mathbf{L}}$. They also assume that the factors between the poses contain a constant diagonal noise covariance; μ and Ψ are constants which depend on this noise model. In their demonstration they show that when the ratio between the angular variance and the position variance is small, these bounds are empirically tight. This case can happen when a navigation agent is equipped with a compass, which reduces the angular noise.

4 Experimental Results

4.1 The Scenario

To demonstrate the advantages of the approach, we applied it to the solution of a highly realistic active-SLAM problem. In this scenario, a robotic agent navigates to a list of goals in an unknown indoor environment. We used the Gazebo simulation engine (Koenig and Howard 2004) to simulate the environment and the robot – Pioneer 3-AT, which is the standard ground robot used in academic research worldwide. The robot is equipped with a lidar sensor, Hokuyo UST-10LX. These components can be seen in Fig. 4. Despite examining a 2D navigation scenario here, our method does not impose any restrictions on the robot’s pose size nor on its state structure.

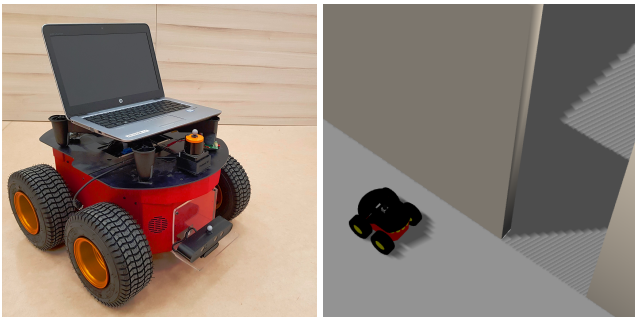


Figure 4. Pioneer 3-AT robot – real and in simulation. A lidar sensor, Hokuyo UST-10LX, is visible.

We use the pose-SLAM paradigm, meaning, the agent’s state $\mathbf{X}_k \doteq (x_0^T, \dots, x_k^T)^T$ consists of poses kept along its entire trajectory. Each of these poses consists of three variables, representing the position and orientation. Our

approach is highly relevant in this case, in which the state size grows quickly as the navigation progresses, making the planning more computationally-challenging. The belief over the state is represented as a factor graph, and implemented using the GTSAM C++ library (Dellaert 2012). When adding a new pose to the graph, the sensor scans the environment in a range of 30 meters, and provides a point-cloud of it. This point-cloud is then matched to scans taken in previous poses using ICP matching (Besl and McKay 1992). If a match is found, a loop-closure factor (constraint) is added between these poses. Motion constraints are also created between every two consecutive poses. Both the observation and motion contain some Gaussian noise, which matches the real hardware’s specs. Robot Operating System (ROS) is used to run and coordinate the system components – state inference, decision making, sensing, etc.

The full map is unknown to the robot, and it is inferred by it using the scans during the navigation. We do, however, use the full map to produce collision-free candidate trajectories. We use the Probabilistic RoadMmap (PRM) algorithm (Kavraki et al. 1996) to sample the map, and then use the K-diverse-paths algorithm (Voss et al. 2015) to build a set \mathcal{U} of trajectories to the current goal. This usage of the map is irrelevant to the demonstration of our method; in our formulation, we consider the candidate actions are given. The complete indoor map is shown in Fig. 5, with the sampled PRM graph on it. Each trajectory matches, of course, a certain control sequence, and is translated to a series of factors and constraints to be added to the prior factor graph. Loop closure constraints are added between poses in the new trajectory, and poses in the previously-executed trajectory, according to their estimated location, i.e. where we expect to add them when executing this trajectory. The corresponding collective Jacobians of the candidate trajectories are constructed as explained in Section 3.1.

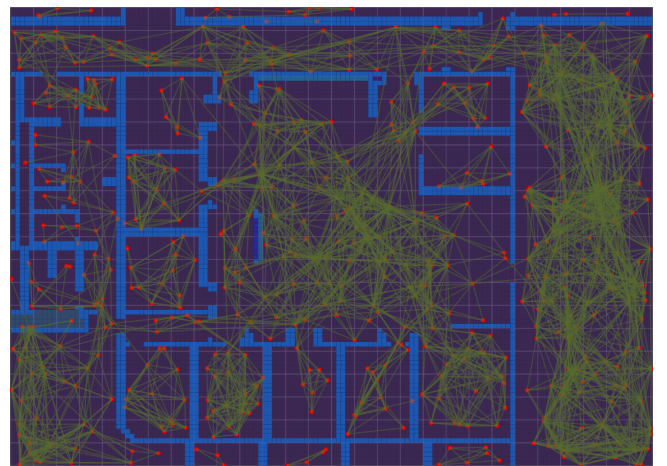


Figure 5. The entire indoor environment from a top view. Walls are colored in light blue. The PRM graph, from which trajectories are built, is colored in red and green. Each square on the map represents a $1\text{m} \times 1\text{m}$ square in reality.

Since all trajectories lead to the goal, we only wish to optimize the “safety” of taking the path. Meaning, keeping the uncertainty of the state low, by preferring a more informative trajectory. We use the aforementioned objective function J from Eq. 23 to compare between candidates.

Session	Prior Size	$\mathcal{P}_{involved}$				$\mathcal{P}_{diagonal}$		
		Uninvolved var. ratio	Run-time	Sparsification time	Non zeros	Run-time	Sparsification time	Non zeros
1	567	46%	-23%	3%	-76%	-55%	1%	-97%
2	762	74%	-34%	4%	-77%	-67%	1%	-98%
3	1182	60%	-66%	1%	-83%	-85%	1%	-99%
4	1269	69%	-70%	2%	-86%	-86%	2%	-99%
5	1341	65%	-67%	2%	-84%	-82%	2%	-99%
6	1392	44%	-52%	<1%	-61%	-80%	<1%	-99%

Table 1. Numerical summary for all sessions. “Uninvolved var. ratio” represents the percentage of uninvolved variables in the prior state. “Run-time” represents the reduction in decision making time in the specified configuration, in comparison to the original problem. “Non zeros” represents the reduction in the number of non-zero entries in the prior information root matrix, after using the sparsification. “Sparsification time” represents the cost of this one-time calculation, out of the entire problem run-time.

Under the “maximum likelihood” assumption, our method is only relevant to the computation of this information-theoretic measure, so for a more convenient discussion, we do not consider other objectives, such as the length of the trajectory.

To cover its list of goals, the robot executes several planning sessions. In each session, the robot is provided with one goal, generates a set of candidate trajectories \mathcal{U} to it, and selects the best candidate by solving a decision problem. The robot completes executing the entire selected trajectory before starting a new planning session to the next goal. To evaluate our method, in each planning session, we solved three decision problems, with each problem using another version of the initial belief. The robot’s original initial belief accounts for the trajectory of poses executed up to that point (the entire inferred state). The other two versions are generated by sparsifying the original belief using Algorithm 1; one with partial sparsification, and one with full sparsification. Overall, in each session, the three configurations of the decision problem are as follows:

1. $\mathcal{P} = (b, \mathcal{U}, J)$ – the original decision problem;
2. $\mathcal{P}_{involved} = (b_{involved}, \mathcal{U}, J)$ – with sparsification of the uninvolved variables – an action consistent problem. We remind again that uninvolved variables correspond to columns of zeros in the collective Jacobians of all candidate actions, as explained in Section 3.2.1.
3. $\mathcal{P}_{diagonal} = (b_{diagonal}, \mathcal{U}, J)$ – with sparsification of all variables, leading to a diagonal information matrix, but not necessarily action consistent.

For each configuration, we measured the objective function calculation time for each candidate action, along with the one-time calculation of the sparsification itself for the latter two. On the whole, in each planning session, we measure the total decision making time for each of the three configurations. For a fair comparison of the problems, the objective calculation was detached from the factor graph. From GTSAM, we extracted the information root matrix of the initial belief, and the collective Jacobians corresponding to (the factors added by) each candidate trajectory. Then, using Algorithm 1, we created the two additional versions of the prior matrix, as detailed before. For each of the three decision problems, i.e. using each version of the prior information root matrix, the corresponding posterior root matrices could then be inferred, as explained in Eq. 25 (via QR update); finally, we easily extracted the determinant of these triangular matrices to calculate the objective function.

At the end of each session, we applied the action selected by the configuration 1. Of course, in a real application we would only solve the problem using a single configuration; here we present a comparison of the results for different configurations. We also did not invest in smart selection of variables for sparsification, as even full sparsification achieved very accurate results.

4.2 Results

In the following section we present and analyze the results from a sequence of six planning sessions. Of course, these sessions took place after the robot had already executed a certain trajectory in the environment, in order to build a state in a substantial size, and a map; if the prior state is empty, examining its sparsification is vain. Figs. 6-10 showcase a summary of each of planning sessions, and contain several components:

(a) A screenshot of the scenario, which includes: the map estimation (blue occupancy grid); the current estimated position (yellow arrow-head) and goal (yellow circle); the trajectory taken up to that point (thin green line); the candidate trajectories from the current position to the goal (thick lines in various colors); and the selected trajectory (highlighted in bright green).

(b) A comparison of the objective function values of the candidate actions (i.e. trajectories), considering each of the versions of the initial belief: \mathcal{P} with the original belief in red; $\mathcal{P}_{involved}$ with sparsification of the uninvolved variables in blue; and $\mathcal{P}_{diagonal}$ with sparsification of all the variables in green. For scale, the comparison also contains the prior differential entropy, before applying any action. This “prior value” is not affected by the sparsification, and is the same for the three configurations (Eq. 66).

(c) A comparison of the the solution time for the three decision problems. Again, \mathcal{P} in red, $\mathcal{P}_{involved}$ in blue, and $\mathcal{P}_{diagonal}$ in green. The highlighted parts of the blue and green bars mark the cost of the sparsification itself out of the total solution time.

(d) A comparison of the three versions of the triangular information root matrix. The figures indicate non-zero entries in each matrix, i.e. sparsity pattern.

(e) The sparsity pattern of the collective Jacobians of the examined trajectories. Again, uninvolved variables are identified by having columns of zero in all the Jacobians.

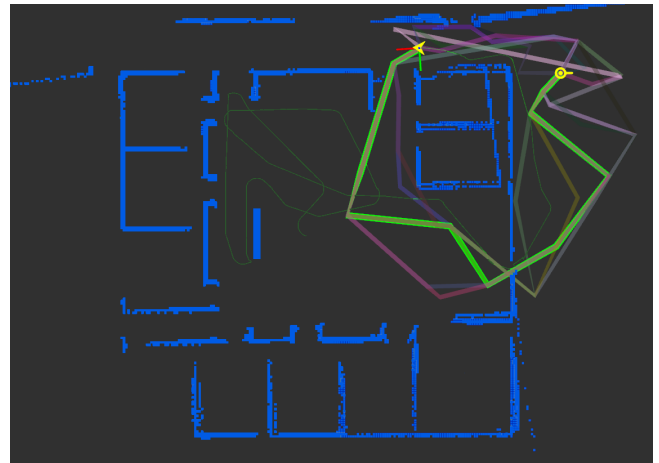
For the first and last sessions we provide an in-depth inspection, including all the components. Since the structure of the belief and Jacobians in all the sessions is similar,

for the intermediate sessions we only present a summarized version, with components (a)-(c). The square root matrix and its approximations, given previously in Fig. 3, are extracted from the third session. Additionally, the numerical data given in the figures is summarized in Table 1. Further data regarding the loss is later given in Table 2.

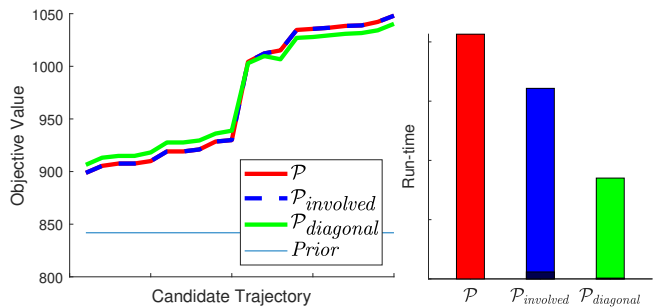
As expected, the sparsification leads to a significant reduction in decision making time. The simplified problem $\mathcal{P}_{diagonal}$ consistently achieves the best performance, followed by $\mathcal{P}_{involved}$, while both are vastly better than the original problem \mathcal{P} . Surely, a higher degree of sparsification (\mathcal{S} containing more variables) leads to a greater improvement in computation time. As discussed in Section 3.2.1, full sparsification of the information root matrix has a particularly low cost – we only need to extract its diagonal. From Table 1 and the run-time comparison bar diagrams, it is clear that the cost of a partial sparsification is also minor in relation to the entire decision making. In some of the diagrams, the highlighted section of the bar, which stands for the cost of the sparsification, is not even visible. Also, since the sparsification cost does not depend on the number of candidate actions, the larger the group of actions is, the less significant the sparsification should become.

We see a correlation between the ratio of uninvolved variables and the reduction in run time with $\mathcal{P}_{involved}$. Variables corresponding to the executed trajectory become involved when a loop closure factor is created between them and a candidate trajectory. Hence, the ratio of uninvolved variables represents the overlap of the candidate trajectories with the previously executed trajectory. In session 1, the executed trajectory is short, resulting in a relatively small state size, and sparse root matrix, since not many loop closures were formed. As the sessions progress, the prior matrix becomes larger and denser, due to new loop closures, as apparent in session 6. In principle, we also notice a correlation between the state size and relative improvement in performance, for both sparsification configurations. Updating the square root factorization, in order to calculate the posterior determinant, has, at worst, cubical complexity in relation to the matrix size. An update to a variable at the beginning of the state (e.g. a loop closure) may force us to recalculate the entire factorization, barring this maximal computational cost. Sparsification of variables reduces the number of elements to update, and thus should be more beneficial when handling larger and denser beliefs.

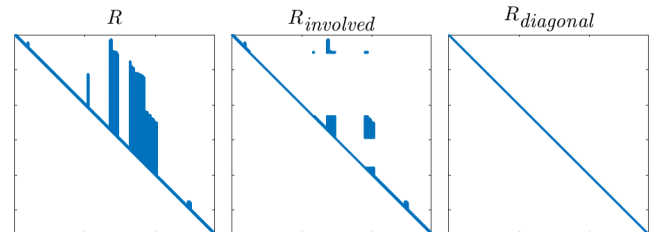
Alongside the undeniable improvement in efficiency, we can also examine the quality of the selected action. According to Theorem 4, not only \mathcal{P} and $\mathcal{P}_{involved}$ are action consistent, but they produce exactly the same objective values. Hence, solving $\mathcal{P}_{involved}$ always leads to the optimal action selection, and induces no loss. $\mathcal{P}_{diagonal}$ is not action consistent with the original problem, therefore maintaining the same action selection is not guaranteed; however, it is evident from Figs. 6-11 that even when sparsifying all the variables using our algorithm, the quality of solution is maintained. Not only does the difference (offset) between the graphs of \mathcal{P} and $\mathcal{P}_{diagonal}$ is slim, but they also maintain a very similar trend, leading to a practically the same action selection and no loss. We emphasize again, that regardless of the selected action, the inference of the next state remains unchanged, as it is done on the original belief.



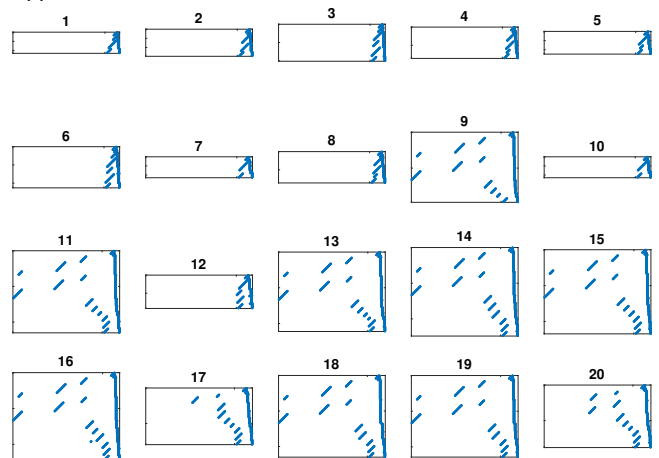
(a) A screenshot of the scenario, which includes: the map estimation (blue occupancy grid); the current estimated position (yellow arrow-head) and goal (yellow circle); the trajectory taken up to that point (thin green line); the candidate trajectories from the current position to the goal (thick lines in various colors); and the selected trajectory (highlighted in bright green).



(b) Objective function comparison. (c) Run-time.

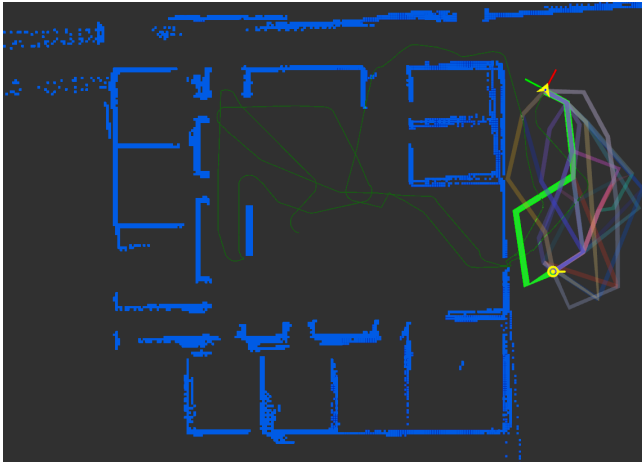


(d) Original prior information root matrix and its sparse approximations.

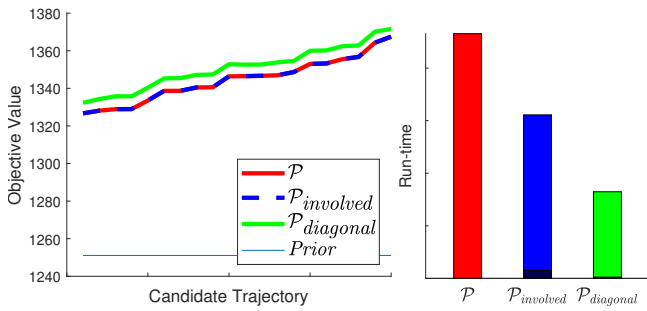


(e) Collective Jacobians of the candidate trajectories.

Figure 6. Results summary for planning session #1.



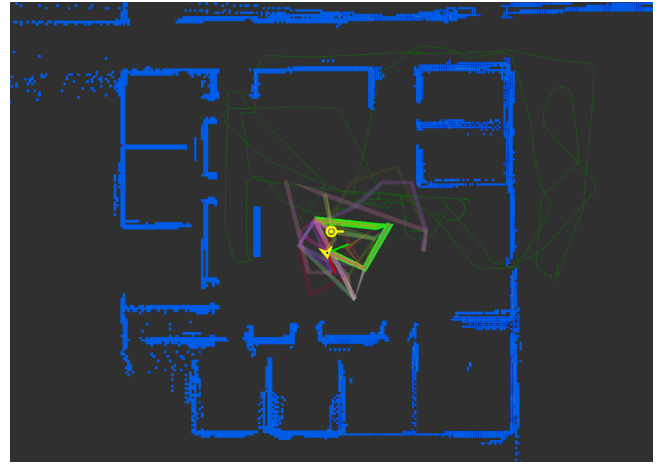
(a) The scenario.



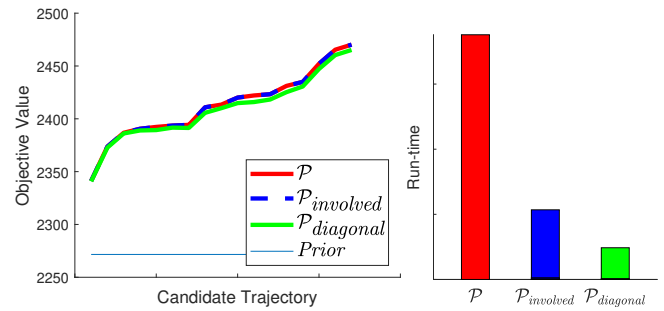
(b) Objective function comparison.

(c) Run-time.

Figure 7. Results summary for planning session #2



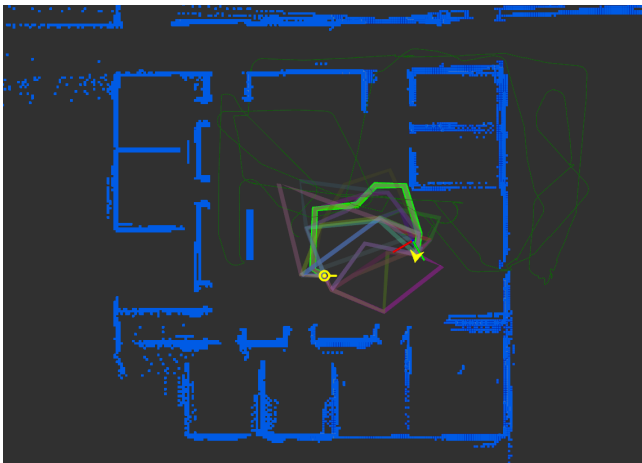
(a) The scenario.



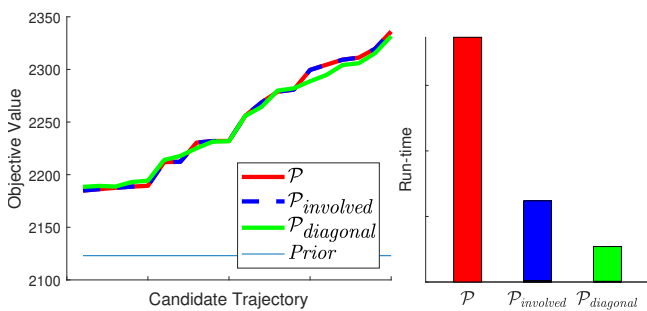
(b) Objective function comparison.

(c) Run-time.

Figure 9. Results summary for planning session #4



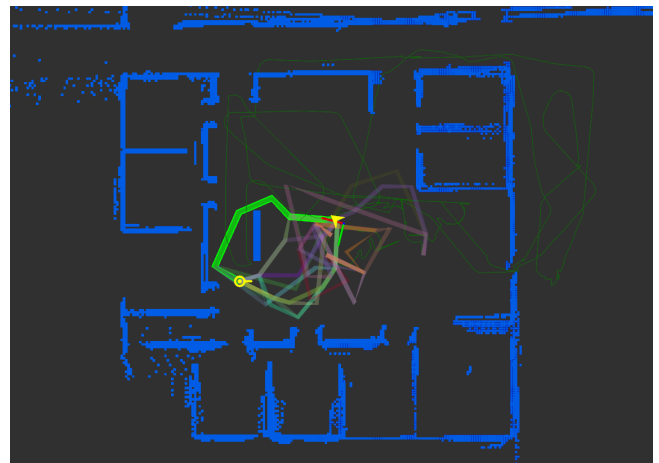
(a) The scenario.



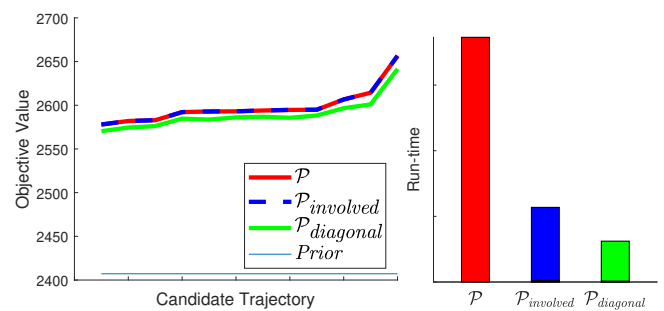
(b) Objective function comparison.

(c) Run-time.

Figure 8. Results summary for planning session #3



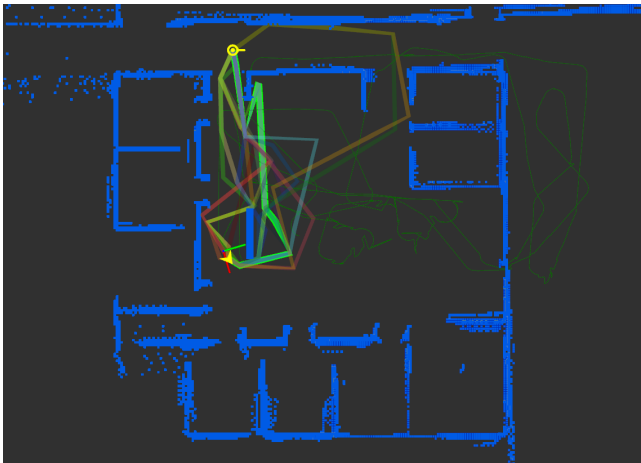
(a) The scenario.



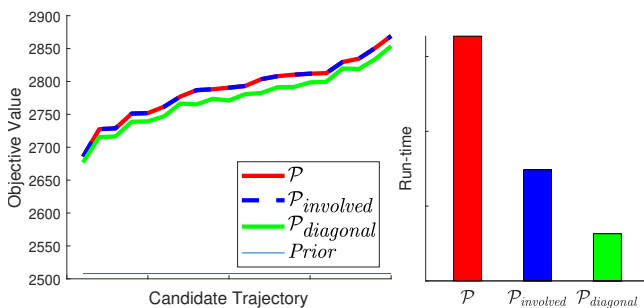
(b) Objective function comparison.

(c) Run-time.

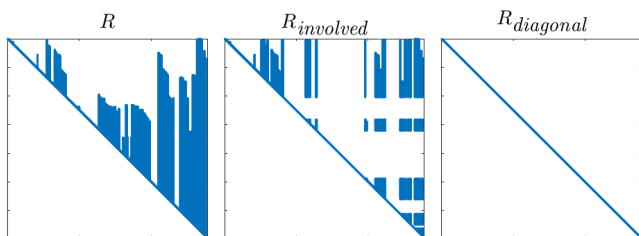
Figure 10. Results summary for planning session #5



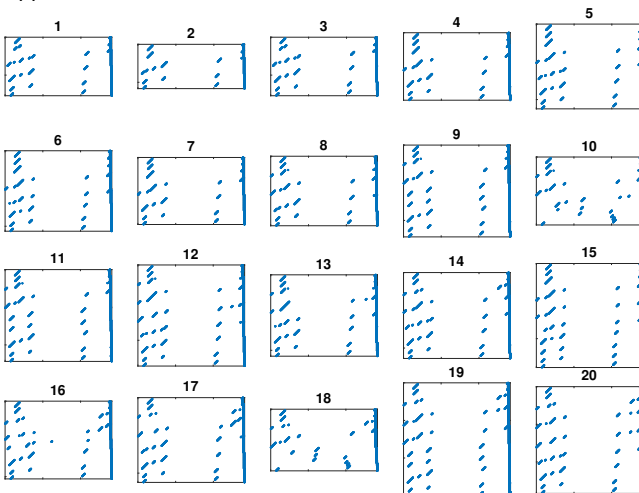
(a) A screenshot of the scenario, which includes: the map estimation (blue occupancy grid); the current estimated position (yellow arrow-head) and goal (yellow circle); the trajectory taken up to that point (thin green line); the candidate trajectories from the current position to the goal (thick lines in various colors); and the selected trajectory (highlighted in bright green).



(b) Objective function comparison. (c) Run-time.



(d) Original prior information root matrix and its sparse approximations.



(e) Collective Jacobians of the candidate trajectories.

Figure 11. Results summary for planning session #6.

4.2.1 Guarantees It is still possible to guarantee the quality of solution, by bounding $loss(\mathcal{P}, \mathcal{P}_{diagonal})$. Obviously no bound should be calculated for $\mathcal{P}_{involved}$, since the loss is guaranteed to be zero. We combine the bounding method previously described in Eq. 8, with the topological bounds from Eq. 46-47. The tightness of these topological bounds depends on the ratio between the angular variance, and the position variance, with which we model the noise in factors between poses; the smaller the angular noise is, in relation to the latter, the tighter the bounds are (as analyzed by Kitanov and Indelman (2019)). Hence, we calculated the loss bound assuming different noise models (different such ratios), and examined their effects. Such change to the noise model has a minor effect on the objective function, since it does not change the sparsity pattern of the matrices; thus, we only present the effect on the inferred loss bound. Bounds, which were calculated assuming different noise ratios, are given in Table 2. The loss and its bounds are brought as a percentage of the maximal approximated objective function value in that session, to allow a correct comparison. In the scenario showcased before, the angular variance to position variance ratio is 0.25:1.

Indeed, changing the noise model has a significant influence on the tightness of the loss bounds. A ratio of 0.01:1 yields a very tight bound. It is not far-fetched that the angular variance would be this low in a navigation scenario, for example, by having a compass, as mentioned before. Raising this ratio results in more conservative bounds, especially in comparison to the exact loss, which is zero. Yet they can still be used to guarantee that the solution stays in an acceptable range. Developing tighter bounding methods for the objective function shall help making these guarantees less conservative.

To clarify, this discussion, alongside any assumptions on the noise or state structure, is only brought in order to examine our ability to provide guarantees, using this specific topological method. It is not essential in any way in order to apply the sparsification and improve the performance.

5 Conclusions

In an attempt to allow efficient solution of decision problems, and specifically belief space planning (BSP) problems, we introduced a new solution paradigm. Its impact is intended to be both conceptual and practical. Conceptually, we suggest that the planning, i.e. identification of the best candidate action, can be done using simplified representations or abstractions, without affecting the accuracy of the maintained state. After selecting the best candidate, it should be applied on the original state. On top of that, we presented the $loss$ as a quality of solution measure for the simplification, and demonstrated how it can be bounded, in order to provide guarantees. We recognized that when the simplification maintains action consistency, i.e. the trend of the objective function, there is no loss. Practically, when applying the paradigm to BSP problems, planning can be conducted considering a sparse approximation of the prior belief.

As a part of this paradigm, we provided a scalable algorithm for generation of such sparse approximations. This versatile algorithm can generate approximations of different

Session	$loss(\mathcal{P}, \mathcal{P}_{involved})$	$loss(\mathcal{P}, \mathcal{P}_{diagonal})$	$loss(\mathcal{P}, \mathcal{P}_{diagonal})$ bound – 0.01:1	$loss(\mathcal{P}, \mathcal{P}_{diagonal})$ bound – 0.25:1	$loss(\mathcal{P}, \mathcal{P}_{diagonal})$ bound – 0.85:1
1	0%	0%	2%	16%	46%
2	0%	0%	2%	16%	47%
3	0%	0%	1%	13%	39%
4	0%	0%	1%	15%	43%
5	0%	0%	1%	16%	43%
6	0%	0%	1%	15%	41%

Table 2. The exact loss induced by the two simplified configurations, alongside the bounds on the loss (of the diagonal configuration), for different noise models. The specified ratio for each bound represents the ratio between the angular variance and the position variance. No bound is calculated for the other configuration, since it is guaranteed to induce no loss. The loss and its bounds are brought as a percentage of the maximal approximated value in that session.

degrees, based on the selection of variables for sparsification. Specifically, by identifying uninvolved variables, we can provide an action consistent approximation, with no influence on the action selection. As explained in Section 3.2.2, our sparsification approach is original and intuitive. We presented an in-depth study of our approach in a highly realistic active-SLAM simulation. We showed that using this sparsification of the uninvolved variables, planning time can be significantly reduced, while guaranteeing no loss in the quality of solution. We then showed that planning time can be reduced even further, using full sparsification, for which, in practice, we experienced no loss in the quality of solution as well. Nonetheless, in that case, we demonstrated how the theoretical loss can be bounded.

The proposed novel paradigm offers many possible future research directions. In general, other sparsification methods, besides the provided algorithm, can be used in similar ways; however, their impact on the action selection should be examined. Existing POMDP solution methods can be evaluated with our theoretical framework, to provide a standard comparison tool for measuring the accuracy of planning algorithms. Also, this framework can be used to develop a scheme for elimination of candidate actions; in fact, we have already developed a proof of concept for this idea (Elimelech and Indelman 2017b). We can also examine other simplification methods, such as altering the action set or the objective function. Developing simplification methods for more general beliefs, such as multi-modal Gaussians, can hold important practical significance. Derivation of tighter loss bounds is also of interest. Overall, with the versatility of these ideas, we expect the approach to yield a substantial contribution to the research community.

6 Acknowledgments

The authors would like to acknowledge Dr. Andrej Kitanov from the Faculty of Aerospace Engineering at the Technion - Israel Institute of Technology, for insightful discussions concerning Section 3.2.4, and his assistance with implementing the simulation.

7 Declaration of Conflicting Interest

The authors declare that there is no conflict of interest.

8 Funding

This work was supported by the Israel Science Foundation (grant 351/15).

References

- Besl, P. and McKay, N. (1992), ‘A method for registration of 3-D shapes’, *IEEE Trans. Pattern Anal. Machine Intell.* **14**(2).
- Bopardikar, S. D., Englot, B., Speranzon, A. and van den Berg, J. (2016), ‘Robust belief space planning under intermittent sensing via a maximum eigenvalue-based bound’, *IJRR* **35**(13), 1609–1626.
- Boyen, X. and Koller, D. (1998), Tractable inference for complex stochastic processes, in ‘Proc. 14th Conf. on Uncertainty in AI (UAI)’, Madison, WI, pp. 33–42.
- Bryson, M. and Sukkarieh, S. (2008), ‘Observability analysis and active control for airborne SLAM’, *IEEE Trans. Aerosp. Electron. Syst.* **44**, 261–280.
- Carlevaris-Bianco, N. and Eustice, R. M. (2014), Conservative edge sparsification for graph slam node removal, in ‘IEEE Intl. Conf. on Robotics and Automation (ICRA)’, pp. 854–860.
- Carlevaris-Bianco, N., Kaess, M. and Eustice, R. M. (2014), ‘Generic node removal for factor-graph SLAM’, *IEEE Trans. Robotics* **30**(6), 1371–1385.
- Chaves, S. M. and Eustice, R. M. (2016), Efficient planning with the Bayes tree for active SLAM, in ‘Intelligent Robots and Systems (IROS), 2016 IEEE/RSJ International Conference on’, IEEE, pp. 4664–4671.
- Davis, T., Gilbert, J., Larimore, S. and Ng, E. (2004), ‘A column approximate minimum degree ordering algorithm’, *ACM Trans. Math. Softw.* **30**(3), 353–376.
- Dellaert, F. (2012), Factor graphs and GTSAM: A hands-on introduction, Technical Report GT-RIM-CP&R-2012-002, Georgia Institute of Technology.
- Dellaert, F. and Kaess, M. (2006), ‘Square Root SAM: Simultaneous localization and mapping via square root information smoothing’, *Intl. J. of Robotics Research* **25**(12), 1181–1203.
- Du, J., Carlone, L., M. Kaouk Ng, Bona, B. and Indri, M. (2011), A comparative study on active SLAM and autonomous exploration with particle filters, in ‘Proc. of the IEEE/ASME Int. Conf. on Advanced Intelligent Mechatronics’, pp. 916–923.
- Elimelech, K. and Indelman, V. (2017a), Consistent sparsification for efficient decision making under uncertainty in high dimensional state spaces, in ‘IEEE Intl. Conf. on Robotics and Automation (ICRA)’.
- Elimelech, K. and Indelman, V. (2017b), Fast action elimination for efficient decision making and belief space planning using bounded approximations, in ‘Proc. of the Intl. Symp. of Robotics Research (ISRR)’.

- Elimelech, K. and Indelman, V. (2017c), Scalable sparsification for efficient decision making under uncertainty in high dimensional state spaces, in 'IEEE/RSJ Intl. Conf. on Intelligent Robots and Systems (IROS)'.
- Frey, K. M., Steiner, T. J. and How, J. P. (2017), 'Complexity analysis and efficient measurement selection primitives for high-rate graph slam', *arXiv preprint arXiv:1709.06821*.
- Hämmerlin, G. and Hoffmann, K.-H. (2012), *Numerical mathematics*, Springer Science & Business Media.
- Harville, D. A. (1998), 'Matrix algebra from a statistician's perspective', *Technometrics* **40**(2), 164–164.
- Hsiung, J., Hsiao, M., Westman, E., Valencia, R. and Kaess, M. (2018), Information sparsification in visual-inertial odometry, in 'IEEE/RSJ Intl. Conf. on Intelligent Robots and Systems (IROS)', pp. 1146–1153.
- Huang, G., Kaess, M. and Leonard, J. (2012), Consistent sparsification for graph optimization, in 'Proc. of the European Conference on Mobile Robots (ECMR)', pp. 150–157.
- Indelman, V. (2015), Towards information-theoretic decision making in a conservative information space, in 'American Control Conference', pp. 2420–2426.
- Indelman, V. (2016), 'No correlations involved: Decision making under uncertainty in a conservative sparse information space', *IEEE Robotics and Automation Letters (RA-L)* **1**(1), 407–414.
- Indelman, V., Carlone, L. and Dellaert, F. (2015), 'Planning in the continuous domain: a generalized belief space approach for autonomous navigation in unknown environments', *Intl. J. of Robotics Research* **34**(7), 849–882.
- Kaess, M., Johannsson, H., Roberts, R., Ila, V., Leonard, J. and Dellaert, F. (2012), 'iSAM2: Incremental smoothing and mapping using the Bayes tree', *Intl. J. of Robotics Research* **31**, 217–236.
- Karaman, S. and Frazzoli, E. (2011), 'Sampling-based algorithms for optimal motion planning', *Intl. J. of Robotics Research* **30**(7), 846–894.
- Kavraki, L., Svestka, P., Latombe, J.-C. and Overmars, M. (1996), 'Probabilistic roadmaps for path planning in high-dimensional configuration spaces', *IEEE Trans. Robot. Automat.* **12**(4), 566–580.
- Khosoussi, K., Giamou, M., Sukhatme, G. S., Huang, S., Dissanayake, G. and How, J. P. (2018), 'Reliable graph topologies for SLAM', *Intl. J. of Robotics Research*.
- Kim, A. and Eustice, R. M. (2014), 'Active visual SLAM for robotic area coverage: Theory and experiment', *Intl. J. of Robotics Research* **34**(4-5), 457–475.
- Kitanov, A. and Indelman, V. (2019), 'Towards online global optimality guarantees for topological belief space planning', *IEEE Robotics and Automation Letters (RA-L)*. submitted.
- Koenig, N. and Howard, A. (2004), Design and use paradigms for gazebo, an open-source multi-robot simulator, in 'IEEE/RSJ Intl. Conf. on Intelligent Robots and Systems (IROS)'.
- Kopitkov, D. and Indelman, V. (2017), 'No belief propagation required: Belief space planning in high-dimensional state spaces via factor graphs, matrix determinant lemma and reuse of calculation', *Intl. J. of Robotics Research* **36**(10), 1088–1130.
- Kretschmar, H. and Stachniss, C. (2012), 'Information-theoretic compression of pose graphs for laser-based SLAM', *Intl. J. of Robotics Research* **31**(11), 1219–1230.
- Künzi, H.-P. A. (2001), Nonsymmetric distances and their associated topologies: about the origins of basic ideas in the area of asymmetric topology, in 'Handbook of the history of general topology', Springer, pp. 853–968.
- Manski, C. F. (1988), 'Ordinal utility models of decision making under uncertainty', *Theory and Decision* **25**(1), 79–104.
- McAllester, D. A. and Singh, S. (1999), Approximate planning for factored pomdps using belief state simplification, in 'UAI', Morgan Kaufmann Publishers Inc., pp. 409–416.
- Mu, B., Paull, L., Agha-Mohammadi, A.-A., Leonard, J. J. and How, J. P. (2017), 'Two-stage focused inference for resource-constrained minimal collision navigation', *IEEE Trans. Robotics* **33**(1), 124–140.
- Papadimitriou, C. and Tsitsiklis, J. (1987), 'The complexity of markov decision processes', *Mathematics of operations research* **12**(3), 441–450.
- Pineau, J., Gordon, G. J. and Thrun, S. (2006), 'Anytime point-based approximations for large POMDPs.', *J. of Artificial Intelligence Research* **27**, 335–380.
- Platt, R., Tedrake, R., Kaelbling, L. and Lozano-Pérez, T. (2010), Belief space planning assuming maximum likelihood observations, in 'Robotics: Science and Systems (RSS)', Zaragoza, Spain, pp. 587–593.
- Porta, J. M., Vlassis, N., Spaan, M. T. and Poupart, P. (2006), 'Point-based value iteration for continuous pomdps', *J. of Machine Learning Research* **7**, 2329–2367.
- Prentice, S. and Roy, N. (2009), 'The belief roadmap: Efficient planning in belief space by factoring the covariance', *Intl. J. of Robotics Research* **28**(11-12), 1448–1465.
- Roy, N., Gordon, G. J. and Thrun, S. (2005), 'Finding approximate pomdp solutions through belief compression', *J. Artif. Intell. Res.(JAIR)* **23**, 1–40.
- Stachniss, C., Haehnel, D. and Burgard, W. (2004), Exploration with active loop-closing for FastSLAM, in 'IEEE/RSJ Intl. Conf. on Intelligent Robots and Systems (IROS)'.
- Thrun, S., Liu, Y., Koller, D., Ng, A., Ghahramani, Z. and Durrant-Whyte, H. (2004), 'Simultaneous localization and mapping with sparse extended information filters', *Intl. J. of Robotics Research* **23**(7-8), 693–716.
- Van Den Berg, J., Patil, S. and Alterovitz, R. (2012), 'Motion planning under uncertainty using iterative local optimization in belief space', *Intl. J. of Robotics Research* **31**(11), 1263–1278.
- Voss, C., Moll, M. and Kavraki, L. E. (2015), A heuristic approach to finding diverse short paths, in 'IEEE Intl. Conf. on Robotics and Automation (ICRA)', pp. 4173–4179.

A Appendix: Proofs

A.1 Corollary 1

The properties are trivially given from the definition of action consistency.

A.2 Theorem 1

Proof.

Assume f is a monotonously increasing function s.t. for every two actions $a_i, a_j \in \mathcal{A}$

$$f(J_1(\xi_1, a_i)) = J_2(\xi_2, a_i), \quad f(J_1(\xi_1, a_j)) = J_2(\xi_2, a_j), \quad (48)$$

then

$$f(J_1(\xi_1, a_i)) < f(J_1(\xi_1, a_j)) \iff J_2(\xi_2, a_i) < J_2(\xi_2, a_j), \quad (49)$$

Because f is monotonously increasing, then $f(x) < f(y) \iff x < y$, and

$$J_1(\xi_1, a_i) < J_1(\xi_1, a_j) \iff J_2(\xi_2, a_i) < J_2(\xi_2, a_j). \quad (50)$$

Meaning, $(\xi_1, \mathcal{A}, J_1) \simeq (\xi_2, \mathcal{A}, J_2)$.

Now to prove the opposite direction, assume $(\xi_1, \mathcal{A}, J_1) \simeq (\xi_2, \mathcal{A}, J_2)$; hence,

$$J_1(\xi_1, a_i) < J_1(\xi_1, a_j) \iff J_2(\xi_2, a_i) < J_2(\xi_2, a_j). \quad (51)$$

Let us define a new function f on the domain $\{J_1(\xi_1, a) \mid a \in \mathcal{A}\}$ s.t. $f(J_1(\xi_1, a)) \doteq J_2(\xi_2, a)$. Given this definition and the action consistency conditions from Eq. 51, we can conclude that

$$f(J_1(\xi_1, a_i)) < f(J_1(\xi_1, a_j)) \iff J_2(\xi_2, a_i) < J_2(\xi_2, a_j) \iff J_1(\xi_1, a_i) < J_1(\xi_1, a_j). \quad (52)$$

Thus, f is monotonously increasing on its domain. \square

A.3 Corollary 2

Proof.

Both directions are a direct consequence of Theorem 1. Assume $\gamma^*(\mathcal{P}, \mathcal{P}_s) = 0$. Thus, a monotonously increasing balance function f exists s.t. $\gamma(\mathcal{P}, \mathcal{P}_s^f) = 0$. Meaning, for every action $a \in \mathcal{A}$, $f(J_s(\xi_s, a)) = J(\xi, a)$. According to Theorem 1, it is sufficient to prove that $\mathcal{P} \simeq \mathcal{P}_s$.

To prove the opposite direction, assume $\mathcal{P} \simeq \mathcal{P}_s$. Let us define a new function f on the domain $\{J_s(\xi_s, a) \mid a \in \mathcal{A}\}$ s.t. $f(J_s(\xi_s, a)) \doteq J(\xi, a)$. From this definition, $\gamma(\mathcal{P}, \mathcal{P}_s^f) = 0$. Also, according to Theorem 1, this function f is monotonously increasing, and can be used as a balance function, thus $\gamma^*(\mathcal{P}, \mathcal{P}_s) = 0$. \square

A.4 Theorem 2

Proof.

Let us examine three decision problems $\mathcal{P}_1, \mathcal{P}_2, \mathcal{P}_3$, where $\mathcal{P}_i \doteq (\xi_i, \mathcal{A}, J_i)$. First, let us define the notation

$\gamma(\mathcal{P}_i, \mathcal{P}_j, a) \doteq |J_i(\xi_i, a) - J_j(\xi_j, a)|$. Now, for each two problems $\mathcal{P}_i, \mathcal{P}_j$, we mark $a_{ij} \in \mathcal{A}$ as the action, and f_{ij} as the balance function, for which $\gamma^*(\mathcal{P}_i, \mathcal{P}_j) \doteq \gamma(\mathcal{P}_i, \mathcal{P}_j^{f_{ij}}, a_{ij})$ (the values can be chosen arbitrarily from all values which comply to the equation). According to this notation we can conclude:

$$\begin{aligned} & \gamma^*(\mathcal{P}_1, \mathcal{P}_2) + \gamma^*(\mathcal{P}_2, \mathcal{P}_3) \doteq \\ & \gamma(\mathcal{P}_1, \mathcal{P}_2^{f_{12}}, a_{12}) + \gamma(\mathcal{P}_2, \mathcal{P}_3^{f_{23}}, a_{23}) \geq \\ & \gamma(\mathcal{P}_1, \mathcal{P}_2^{f_{12}}, a_{13}) + \gamma(\mathcal{P}_2, \mathcal{P}_3^{f_{23}}, a_{13}) \doteq \\ & |J_1(\xi_1, a_{13}) - f_{12}(J_2(\xi_2, a_{13}))| + \\ & |J_2(\xi_2, a_{13}) - f_{23}(J_3(\xi_3, a_{13}))| \geq \\ & |J_1(\xi_1, a_{13}) - f_{12}(J_2(\xi_2, a_{13})) + \\ & J_2(\xi_2, a_{13}) - f_{23}(J_3(\xi_3, a_{13}))| \doteq (**). \end{aligned} \quad (53)$$

Let us define the following scalar function:

$$F(x) \doteq f_{23}(x) + f_{12}(J_2(\xi_2, a_{13})) - J_2(\xi_2, a_{13}) = f_{23}(x) + \text{constant}. \quad (54)$$

Since f_{23} is a monotonously increasing, so is F , and

$$\begin{aligned} (**) & = |J_1(\xi_1, a_{13}) - F(J_3(\xi_3, a_{13}))| \doteq \\ & \gamma(\mathcal{P}_1, \mathcal{P}_3^F, a_{13}) \geq \\ & \gamma(\mathcal{P}_1, \mathcal{P}_3^{f_{13}}, a_{13}) = \\ & \gamma^*(\mathcal{P}_1, \mathcal{P}_3). \end{aligned} \quad (55)$$

Hence, γ^* satisfies the triangle inequality. \square

A.5 Theorem 3

Proof.

Given any monotonously increasing function f , consider the following false assumption:

$$|J(\xi, a^*) - f(J_s(\xi_s, a_s^*))| > \gamma(\mathcal{P}, \mathcal{P}_s^f) \left[\doteq \max_{a \in \mathcal{A}} |J(\xi, a) - f(J_s(\xi_s, a))| \right]. \quad (56)$$

Consider $J(\xi, a^*) \geq f(J_s(\xi_s, a_s^*))$. By definition $J_s(\xi_s, a_s^*) \geq J_s(\xi_s, a^*)$; from the definition of f we conclude that $J(\xi, a^*) \geq f(J_s(\xi_s, a_s^*)) \geq f(J_s(\xi_s, a^*))$. Hence,

$$\begin{aligned} |J(\xi, a^*) - f(J_s(\xi_s, a_s^*))| & > |J(\xi, a^*) - f(J_s(\xi_s, a^*))|, \\ J(\xi, a^*) - f(J_s(\xi_s, a_s^*)) & > J(\xi, a^*) - f(J_s(\xi_s, a^*)), \\ f(J_s(\xi_s, a^*)) & > f(J_s(\xi_s, a_s^*)), \\ J_s(\xi_s, a^*) & > J_s(\xi_s, a_s^*). \end{aligned} \quad (57)$$

This is a contradiction to the definition of a_s^* . Let us examine the complementary case instead. Consider $f(J_s(\xi_s, a_s^*)) > J(\xi, a^*)$. By definition also $J(\xi, a^*) \geq J(\xi, a_s^*)$; hence,

$$\begin{aligned} |J(\xi, a^*) - f(J_s(\xi_s, a_s^*))| & > |J(\xi, a_s^*) - f(J_s(\xi_s, a_s^*))|, \\ f(J_s(\xi_s, a_s^*)) - J(\xi, a^*) & > f(J_s(\xi_s, a_s^*)) - J(\xi, a_s^*), \\ J(\xi, a_s^*) & > J(\xi, a^*). \end{aligned} \quad (58)$$

This is a contradiction to the definition of a^* . Meaning, in any way the initial false assumption is not possible; therefore,

$$|J(\xi, a^*) - f(J_s(\xi_s, a_s^*))| \leq \gamma(\mathcal{P}, \mathcal{P}_s^f). \quad (59)$$

Now, using this conclusion, and according to the definitions of loss and simplification offset:

$$\begin{aligned} J(\xi, a^*) - f(J_s(\xi_s, a_s^*)) &\leq \gamma(\mathcal{P}, \mathcal{P}_s^f), \\ J(\xi, a^*) - J(\xi, a_s^*) + J(\xi, a_s^*) - f(J_s(\xi_s, a_s^*)) &\leq \gamma(\mathcal{P}, \mathcal{P}_s^f), \\ \text{loss}(\mathcal{P}, \mathcal{P}_s) + J(\xi, a_s^*) - f(J_s(\xi_s, a_s^*)) &\leq \gamma(\mathcal{P}, \mathcal{P}_s^f), \\ \text{loss}(\mathcal{P}, \mathcal{P}_s) &\leq \gamma(\mathcal{P}, \mathcal{P}_s^f) + f(J_s(\xi_s, a_s^*)) - J(\xi, a_s^*), \\ \text{loss}(\mathcal{P}, \mathcal{P}_s) &\leq \gamma(\mathcal{P}, \mathcal{P}_s^f) + |J(\xi, a_s^*) - f(J_s(\xi_s, a_s^*))|, \\ \text{loss}(\mathcal{P}, \mathcal{P}_s) &\leq \gamma(\mathcal{P}, \mathcal{P}_s^f) + \gamma(\mathcal{P}, \mathcal{P}_s^f), \\ \text{loss}(\mathcal{P}, \mathcal{P}_s) &\leq 2 \cdot \gamma(\mathcal{P}, \mathcal{P}_s^f). \end{aligned} \quad (60)$$

Since the final statement is true for any monotonously increasing function f , we may conclude the desired upper bound over the loss,

$$\text{loss}(\mathcal{P}, \mathcal{P}_s) \leq 2 \cdot \gamma^*(\mathcal{P}, \mathcal{P}_s) \quad (61)$$

□

A.6 Corollary 3

Proof.

Let us mark as \mathbf{R}'_s the sparsified root matrix, before permuting the variables back to their original order in line 9 of Algorithm 1. First, we show that applying the reverse permutation $\mathbf{P}^T \square \mathbf{P}$ on \mathbf{R}'_s indeed leads to a square root matrix of the sprse information Λ_s (in the original order):

$$(\mathbf{P}^T \mathbf{R}'_s \mathbf{P})^T (\mathbf{P}^T \mathbf{R}'_s \mathbf{P}) = \mathbf{P}^T \mathbf{R}'_s{}^T \mathbf{R}'_s \mathbf{P} = \mathbf{P}^T \Lambda'_s \mathbf{P} = \Lambda_s, \quad (62)$$

where Λ'_s is the sparsified information matrix, before permuting the variables back.

Now, we want to examine the shape of this root matrix $\mathbf{R}_s \doteq \mathbf{P}^T \mathbf{R}'_s \mathbf{P}$, and show that it is indeed triangular. According to the Algorithm 1, before executing line 9, \mathbf{R}'_s is of the following structure:

$$\mathbf{R}'_s = \left(\begin{array}{c|c} \text{diagonal} & \mathbf{0} \\ \hline \mathbf{0} & \text{triangular} \end{array} \right), \quad (63)$$

where the rows of the diagonal block correspond to the sparsified variables. Without losing generality, we should only prove that applying a permutation of the form $p: (1, \dots, N) \mapsto (2, \dots, i, 1, i+1, \dots, N)$ does not break the triangular form. Hence, assuming \mathbf{P}^T is the permutation matrix matching such p , let us look at

$$\mathbf{R}_s \doteq \mathbf{P}^T \mathbf{R}'_s \mathbf{P} =$$

$$\mathbf{P}^T \left(\begin{array}{c|c} d \in \mathbb{R} & 0 \dots 0 \\ \hline 0 & \text{triangular} \\ \vdots & \\ 0 & \end{array} \right) \mathbf{P} = \left(\begin{array}{c|c|c} 0 & & \\ \vdots & \text{triangular} & * \\ 0 & & \\ \hline d & 0 \dots 0 & 0 \dots 0 \\ \hline 0 & & \\ \vdots & \mathbf{0} & \text{triangular} \\ 0 & & \end{array} \right) \mathbf{P} = \left(\begin{array}{c|c|c} & 0 & \\ \text{triangular} & \vdots & * \\ & 0 & \\ \hline 0 \dots 0 & d & 0 \dots 0 \\ \hline & 0 & \\ \mathbf{0} & \vdots & \text{triangular} \\ & 0 & \end{array} \right). \quad (64)$$

Recursively utilizing this conclusion proves that \mathbf{R}_s is indeed triangular when permuting the sparsified variables back to their original order, as desired. □

A.7 Theorem 4

Proof.

First of all, we notice that variable permutation does not affect the determinant of a matrix:

$$|\mathbf{P} \Lambda \mathbf{P}^T| = |\mathbf{P} \mathbf{P}^T| \cdot |\Lambda| = |\Lambda|, \quad (65)$$

where \mathbf{P} is a (unitary) permutation matrix. Thus, we can prove the theory assuming the variables are already in the required order, i.e. with the uninvolved variables appearing first.

According to lines 5, 7, 8 of the algorithm, matrices \mathbf{R} and \mathbf{R}_s are upper triangular and have the same diagonal, therefore, when $\mathbf{R} \in \mathbb{R}^{n \times n}$,

$$\begin{aligned} |\Lambda| &= |\mathbf{R}^T \mathbf{R}| = |\mathbf{R}|^2 = \\ &= \prod_i^n \mathbf{R}_{ii}^2 = \\ &= |\mathbf{R}_s|^2 = |\mathbf{R}_s^T \mathbf{R}_s| = |\Lambda_s|. \end{aligned} \quad (66)$$

Consider an action $u \in \mathcal{U}$ with a collective Jacobian $\mathbf{U} \in \mathbb{R}^{h \times (n+m)}$, where n is the prior state size, and $(n+m)$ is the posterior state size. Collective Jacobians may include new state variables, and thus require augmentation of the prior (as described in Eq. 18). We use the auxiliary matrix $\mathbf{E}^{(n+m) \times (n+m)}$ which simply contains 1's on the diagonal entries corresponding to variables added in the augmentation. The matrix shall be used to make sure the

prior matrix stays positive semi-definite after augmentation.

$$E_{ij} \doteq \begin{cases} 1 & i = j \text{ and the } i\text{-th variable is firstly} \\ & \text{introduced by the action } a \\ 0 & \text{else} \end{cases} \quad (67)$$

Since variable permutation does not affect the determinant (as shown in Eq. 65), and as new variables are necessarily involved, we can assume the new variables are added to the end of the state. Then,

$$\left| \check{\Lambda} + \alpha \cdot \mathbf{E} \right| = \left| \begin{bmatrix} \Lambda & \mathbf{0} \\ \mathbf{0} & \alpha \cdot \mathbf{I}^{m \times m} \end{bmatrix} \right| = \alpha^m \cdot |\Lambda|. \quad (68)$$

Also, since both the determinant and the matrix inversion (for example, using Cayley-Hamilton method (see Harville 1998)) are linear operations on the elements of a matrix, the following limits are well defined:

$$\lim_{\alpha \rightarrow 0} \left| \check{\Lambda} + \alpha \cdot \mathbf{E} + \mathbf{U}^T \mathbf{U} \right| = \left| \check{\Lambda} + \mathbf{U}^T \mathbf{U} \right|, \quad (69)$$

$$\lim_{\alpha \rightarrow 0} (\check{\Lambda} + \alpha \cdot \mathbf{E})^{-1} = \Lambda^{-1}. \quad (70)$$

Now, let us look at the following progression, in which every statement results from the one following. When the transition is not trivial, justifications are given between the steps.

$$J(b, u) = J(b_s, u) \quad (71)$$

(Definition of J in Eq. 23)

$$\left| \check{\Lambda} + \mathbf{U}^T \mathbf{U} \right| = \left| \check{\Lambda}_s + \mathbf{U}^T \mathbf{U} \right| \quad (72)$$

(From Eq. 69)

$$\lim_{\alpha \rightarrow 0} \left| \check{\Lambda} + \alpha \cdot \mathbf{E} + \mathbf{U}^T \mathbf{U} \right| = \lim_{\alpha \rightarrow 0} \left| \check{\Lambda}_s + \alpha \cdot \mathbf{E} + \mathbf{U}^T \mathbf{U} \right| \quad (73)$$

(Matrix determinant lemma (see Harville 1998))

$$\lim_{\alpha \rightarrow 0} \left| \check{\Lambda} + \alpha \cdot \mathbf{E} \right| \cdot \left| \mathbf{I} + \mathbf{U}(\check{\Lambda} + \alpha \cdot \mathbf{E})^{-1} \mathbf{U}^T \right| = \lim_{\alpha \rightarrow 0} \left| \check{\Lambda}_s + \alpha \cdot \mathbf{E} \right| \cdot \left| \mathbf{I} + \mathbf{U}(\check{\Lambda}_s + \alpha \cdot \mathbf{E})^{-1} \mathbf{U}^T \right| \quad (74)$$

(From Eq. 68)

$$\lim_{\alpha \rightarrow 0} \alpha^m \cdot |\Lambda| \cdot \left| \mathbf{I} + \mathbf{U}(\check{\Lambda} + \alpha \cdot \mathbf{E})^{-1} \mathbf{U}^T \right| = \lim_{\alpha \rightarrow 0} \alpha^m \cdot |\Lambda_s| \cdot \left| \mathbf{I} + \mathbf{U}(\check{\Lambda}_s + \alpha \cdot \mathbf{E})^{-1} \mathbf{U}^T \right| \quad (75)$$

(From Eq. 66)

$$\lim_{\alpha \rightarrow 0} \alpha^m \cdot \left| \mathbf{I} + \mathbf{U}(\check{\Lambda} + \alpha \cdot \mathbf{E})^{-1} \mathbf{U}^T \right| = \lim_{\alpha \rightarrow 0} \alpha^m \cdot \left| \mathbf{I} + \mathbf{U}(\check{\Lambda}_s + \alpha \cdot \mathbf{E})^{-1} \mathbf{U}^T \right| \quad (76)$$

$$\lim_{\alpha \rightarrow 0} \left| \mathbf{I} + \mathbf{U}(\check{\Lambda} + \alpha \cdot \mathbf{E})^{-1} \mathbf{U}^T \right| = \lim_{\alpha \rightarrow 0} \left| \mathbf{I} + \mathbf{U}(\check{\Lambda}_s + \alpha \cdot \mathbf{E})^{-1} \mathbf{U}^T \right| \quad (77)$$

(Determinant is a linear operation on the elements of a matrix)

$$\left| \mathbf{I} + \mathbf{U} \left(\lim_{\alpha \rightarrow 0} (\check{\Lambda} + \alpha \cdot \mathbf{E})^{-1} \right) \mathbf{U}^T \right| = \left| \mathbf{I} + \mathbf{U} \left(\lim_{\alpha \rightarrow 0} (\check{\Lambda}_s + \alpha \cdot \mathbf{E})^{-1} \right) \mathbf{U}^T \right| \quad (78)$$

(From Eq. 70)

$$\left| \mathbf{I} + \mathbf{U} \check{\Lambda}^{-1} \mathbf{U}^T \right| = \left| \mathbf{I} + \mathbf{U} \check{\Lambda}_s^{-1} \mathbf{U}^T \right| \quad (79)$$

$$\left| \mathbf{I} + \mathbf{U} \check{\mathbf{R}}^{-1} (\check{\mathbf{R}}^{-1})^T \mathbf{U}^T \right| = \left| \mathbf{I} + \mathbf{U} \check{\mathbf{R}}_s^{-1} (\check{\mathbf{R}}_s^{-1})^T \mathbf{U}^T \right| \quad (80)$$

$$\left| \mathbf{I} + (\mathbf{U} \check{\mathbf{R}}^{-1}) (\mathbf{U} \check{\mathbf{R}}^{-1})^T \right| = \left| \mathbf{I} + (\mathbf{U} \check{\mathbf{R}}_s^{-1}) (\mathbf{U} \check{\mathbf{R}}_s^{-1})^T \right| \quad (81)$$

$$\mathbf{U} \check{\mathbf{R}}^{-1} = \mathbf{U} \check{\mathbf{R}}_s^{-1} \quad (82)$$

We recall that all uninvolved variables appear first in the state vector; hence, we can use a block representation of $\check{\mathbf{R}}$, and apply the block inverse formula (and similarly to $\check{\mathbf{R}}_s$) (see Harville 1998):

$$\check{\mathbf{R}}^{-1} \doteq \begin{bmatrix} \check{\mathbf{R}}_{11}^{-1} & \check{\mathbf{R}}_{12} \\ \mathbf{0} & \check{\mathbf{R}}_{22} \end{bmatrix}^{-1} = \begin{bmatrix} \mathbf{R}_{11}^{-1} & -\check{\mathbf{R}}_{11}^{-1} \check{\mathbf{R}}_{12} \check{\mathbf{R}}_{22}^{-1} \\ \mathbf{0} & \check{\mathbf{R}}_{22}^{-1} \end{bmatrix}, \quad (83)$$

where the uninvolved variables correspond to the rows of \mathbf{R}_{11} . Since we only sparsify elements from these rows, only blocks $\check{\mathbf{R}}_{11}, \check{\mathbf{R}}_{12}$ are affected by the sparsification, and $\check{\mathbf{R}}_{22} = \check{\mathbf{R}}_{s22}$. We also know that columns of the \mathbf{U} corresponding to uninvolved variables are zero by definition, thus \mathbf{U} can also be written in a matching block representation $\mathbf{U} \doteq \begin{bmatrix} \mathbf{0} & \mathbf{U}_{12} \end{bmatrix}$. Overall,

$$\mathbf{U} \check{\mathbf{R}}^{-1} = \begin{bmatrix} \mathbf{0} & \mathbf{U}_{12} \end{bmatrix} \begin{bmatrix} \mathbf{R}_{11}^{-1} & -\check{\mathbf{R}}_{11}^{-1} \check{\mathbf{R}}_{12} \check{\mathbf{R}}_{22}^{-1} \\ \mathbf{0} & \check{\mathbf{R}}_{22}^{-1} \end{bmatrix} = \begin{bmatrix} \mathbf{0} & \mathbf{U}_{12} \end{bmatrix} \begin{bmatrix} \mathbf{R}_{s11}^{-1} & -\check{\mathbf{R}}_{s11}^{-1} \check{\mathbf{R}}_{s12} \check{\mathbf{R}}_{s22}^{-1} \\ \mathbf{0} & \check{\mathbf{R}}_{s22}^{-1} \end{bmatrix} = \mathbf{U} \check{\mathbf{R}}_s^{-1}. \quad (84)$$

Thus, Eq. 82 and all leading equations are true, and $J(b, u) = J(b_s, u), \forall u \in \mathcal{U}$.